

# Bound-Based Power Optimization for Multi-Hop Heterogeneous Wireless Industrial Networks Under Statistical Delay Constraints

Neda Petreska<sup>a</sup>, Hussein Al-Zubaidy<sup>b</sup>, Rudi Knorr<sup>a</sup>, James Gross<sup>c</sup>

<sup>a</sup>*Fraunhofer Institute for Embedded Systems and Communication Technologies ESK, Munich, Germany*

<sup>b</sup>*School of Information Technology (ITE), Halmstad University, Halmstadt, Sweden*

<sup>c</sup>*School of Electrical Engineering, KTH Royal Institute of Technology, Stockholm, Sweden*

---

## Abstract

The noticeably increased deployment of wireless networks for battery-limited industrial applications in recent years highlights the need for tractable performance analysis methodologies as well as efficient QoS-aware transmit power management schemes. In this work, we seek to combine several important aspects of such networks, i.e., multi-hop connectivity, channel heterogeneity and the queuing effect, in order to address these needs. We design delay-bound-based algorithms for transmit power minimization and network lifetime maximization of multi-hop heterogeneous wireless networks using our previously developed stochastic network calculus approach for performance analysis of a cascade of buffered wireless fading channels. Our analysis shows an overall transmit power saving of up to 95% compared to a fixed power allocation scheme in case when the service is modeled via a Shannon capacity. For a more realistic set-up, we evaluate the performance of the suggested algorithm in a WirelessHART network, which is a widely used communication standard for industrial process automation applications. We find that link heterogeneity can significantly reduce network lifetime when no efficient power management is applied. Using extensive simulation study we further show that the proposed bound-based power allocation performs reasonably well compared to the real optimum, especially in the case of WirelessHART networks.

*Keywords:* stochastic network calculus, wireless sensor networks, multi-hop, heterogeneous networks, end-to-end delay bound, power minimization, industrial networks, WirelessHART

---

*Email addresses:* [neda.petreska@esk.fraunhofer.de](mailto:neda.petreska@esk.fraunhofer.de) (Neda Petreska), [hussain.al-zubaidy@hh.se](mailto:hussain.al-zubaidy@hh.se) (Hussein Al-Zubaidy), [rudi.knorr@esk.fraunhofer.de](mailto:rudi.knorr@esk.fraunhofer.de) (Rudi Knorr), [james.gross@ee.kth.se](mailto:james.gross@ee.kth.se) (James Gross)

## 1. Introduction

In recent years, wireless networking solutions are increasingly being deployed to many new domains such as vehicular networks, machine-to-machine (M2M) communication, home automation, industrial settings and the smart grid. Applications in these areas often require novel combinations of delay and reliability constraints, while on the other hand relying on battery-driven wireless systems. One area where these aspects are especially important is the area of wireless industrial networks, in particular, process automation. Process automation comprises the area of process sensing, control and diagnostics. Target application areas can be found, for example, in refineries, food and chemical industries. Typical process automation applications have Quality-of-Service (QoS) demands with deadlines in the order of hundreds of milliseconds and maximum outage probabilities (with respect to the deadlines) in the order of  $10^{-3}$  to  $10^{-4}$  [1]. At the same time, many of these applications correspond to factory sites which can span over quite a wide range of distances, varying from few meters up to few kilometers. Battery-driven wireless sensors and actuators are mainly applied in these scenarios due to their flexible placement possibilities. Of particular relevance to this work is the tendency of modern industrial solutions to deploy *multi-hop topologies* in order to bridge larger distances without necessarily shortening the lifetime of battery-powered nodes. This poses a significant challenge to existing research efforts to determine the optimal transmit power allocation in such networks. Due to the fact that transmit power is one of the main energy consumers in a wireless device [2], an adaptive transmit power management has the potential to improve battery lifetime in addition to other techniques, such as hardware design, load balancing and transceiver state management [3].

Nevertheless, when it comes to dependable industrial and machine-to-machine applications, transmit power management is challenging as it has to factor in not only the time-varying transmission rate of the wireless channel due to fading, but also latency and reliability constraints. This necessitates a trade-off between power consumption at each node and the physical channel transmit rate, which potentially (due to time variability) leads to a queue build-up at that node. Although transmit power management under QoS requirements has been addressed for single-hop communications [2, 4, 5, 6], power management under stochastic queuing constraints for heterogeneous multi-hop wireless networks remains, to date, an open problem. Solving this problem is the focus of this work. In order to do so, we first need to mathematically express the queuing performance of the wireless network in terms of the transmit power, the fading environment and the used transmission technology/protocols. We then pursue towards solving this expression for the optimal power allocation under given latency and reliability constraints. Unfortunately, an *exact* expression for the performance of heterogeneous multi-hop wireless networks is not tractable so far. Nevertheless, recent advancements in stochastic network calculus [7, 8] enable us to derive probabilistic delay bounds for heterogeneous networks.

Based on this insight, in this work we develop an analytical model for the

performance of heterogeneous multi-hop wireless networks. Using an approach that we developed previously [8], we provide a closed-form expression for the end-to-end probabilistic delay bound. Using this analytical expression, we propose a bound-based optimal power allocation algorithm that minimizes transmit power while maintaining a bound on the delay performance. It is worth noting that optimizing the bound may result in a different operating point (in terms of power allocation per link, for instance) than the true system optimum. However, since up to date no tractable analytical model which optimizes the real operating point of a system exist, we opt towards a bound-based alternative in order to provide an analytical solution of the above described problem.

Taking this into account, we will answer the following essential questions:

1. Is it feasible to provide a bound-based optimal power allocation along a multi-hop path consisting of heterogeneous wireless fading channels under statistical delay constraints? If so, under which conditions?
2. How would such power allocation scheme look like?
3. How good is such bound-based optimal power allocation scheme and how well does it perform compared to the real optimum?

In this paper, we study the structure of the derived end-to-end delay bound and prove some of its important properties for optimization such as *convexity and monotonicity of the delay kernel*, which we define in Section 3. This addresses the first question and enables us to develop a power minimization algorithm for optimal power allocation in a wireless multi-hop path under statistical end-to-end delay constraints.

To address the second question, we use the derived closed-form solution from [8] for the end-to-end delay bound for heterogeneous multi-hop wireless networks to develop two optimization algorithms: (i) a *bound-based power-minimization algorithm* and (ii) a *bound-based network lifetime maximization algorithm*. The first algorithm determines the minimum required transmit power at each hop, such that a given statistical delay bound (which encompasses both latency and reliability) is not violated. The second algorithm determines the allocation of transmit power among all transmitters along the respective path such that for given initial energy levels (e.g., battery charge per intermediate transmitter), the network lifetime is maximized given that the designated statistical delay constraint is not violated. While the first algorithm is suitable for energy efficient networks where energy levels can be replenished (i.e., recharging their batteries is possible), the second is more useful for wireless sensor network applications, especially, for remote area deployment where battery recharging is not possible. This motivated the development of the two separate algorithms. Although the two algorithms may result in the same power allocation scheme for the homogeneous case (assuming identical fading distribution and same initial energy levels for all hops), this is obviously not the case for heterogeneous networks, which are the point of our interest.

To address the third question, we first recognize that optimizing a statistical bound on the delay may differ from optimizing the exact expression for the delay violation probability. Nevertheless, due to the lack of such exact expression at

the time being (and for the foreseeable future, due to the intractability of the analysis in this case), we opt to use the (more tractable) statistical delay bound for our analysis and optimization instead. In this case, it is important to quantify the optimality gap in energy efficiency of the bound-based algorithms compared to the real optimum, which we obtain by simulations. In Section 5 we provide an extensive numerical study to address this point. We show that in many cases of link heterogeneity our algorithm provides a sufficient estimate on the optimal transmit power per node, at the same time avoiding the need for extensive and time-consuming system optimization using simulations.

In the remainder of this section, we present a literature survey of related work, and then list the main contributions of this work. We first discuss related work with respect to general end-to-end transmit power management schemes, then we discuss research papers that deal with end-to-end queuing performance.

### 1.1. Transmit Power Management

Power management under *simplified* end-to-end throughput constraints has been often addressed before [9, 10, 11, 12, 13]. However, none of these works considers queuing effects. For instance, [9] describes a cross-layer design framework, minimizing the total transmit power subject to a minimal end-to-end payload rate valid for all links and maximal bit error rate (BER) requirements per session. The authors use heuristics to determine the transmit power per node. [10] minimizes the total average transmit power under the constraint of providing a minimum average data rate per link. The authors propose an algorithm for optimal link scheduling and power control policy. They also extend this to a routing algorithm, which uses the algorithms' output as a routing metric. They show that the optimal power policy chooses one of two actions, transmitting at peak power or not transmitting at all. Transmit power control in multi-hop networks with respect to the best possible video quality at the receiver is presented in [11]. For this purpose, the authors maximize the peak signal-to-noise ratio and minimize the end-to-end video distortion, which is a function of the end-to-end bit error probability. Results show that power control does not degrade the video quality significantly.

With respect to power management and end-to-end multi-hop performance, two works are perhaps closest to our contribution. First, [14] presents a tradeoff between the average transmit power and a corresponding queuing-delay bound for a multiuser cellular network, multi-hop and point-to-point communication. The authors propose a resource allocation scheme to minimize power consumption subject to statistical delay QoS, given as a queue-length decay rate, jointly determined from the effective bandwidth of the arrival traffic and the effective capacity of the wireless channel. The numerical analysis shows that it is possible to achieve stringent QoS guarantee with little power increase compared to the power needed for loose delay constraints. However, the discussed multi-hop scenario assumes an amplify-and-forward scheme, and therefore does not consider queuing at the intermediate nodes. Second, in [15] the authors present a joint routing and power allocation policy for a wireless multi-hop network with time-varying channels that stabilizes the system and provides bounded average delay

guarantees. The optimal power allocation in both proposed schemes, defined as distributed and centralized control algorithm, is determined under pre-defined stability condition, i.e., for input rates which are strictly inside the network capacity region. It is shown that the derived delay bounds grow asymptotically in the size of the network and a parameter that describes the distance between the arrival rates and the capacity region boundary. The numerical results illustrate the advantage of exploiting channel state and queue backlog. The work, however, covers queuing by focusing mainly on a stability condition and does not consider quantiles on the end-to-end delay.

### 1.2. *Queuing Analysis of Wireless Networks*

From a queuing-theoretic perspective, significant problems arise when trying to characterize quantiles on the end-to-end delay performance of a wireless multi-hop network. Classical models for queuing networks typically only allow the analysis of the average delay. In contrast, the theory of network calculus enables an analysis of delay quantiles via bounds on the arrival and service rather than focusing on the average behaviour. In particular, stochastic network calculus [16] has shown to be especially useful for characterizing traffic arrivals and network service of wireless multi-hop networks. While there are many works addressing performance guarantees over wireless fading channels using this theoretical framework [17, 18, 19, 20, 21, 22, 23, 24], none of them resolve the question on end-to-end delay bounds over heterogeneous fading channels. Attempts in that direction are presented in [21] and [18]. However, while the first one does not provide a closed-form expression for the end-to-end service curve for wireless fading channels, the complexity of the MGF-based framework presented in [18] grows very fast when considering a heterogeneous multi-hop path and results in mathematically intractable expressions. Furthermore, the usage of the Gilbert-Elliott two-state channel model in [20] limits the accuracy of the fading model description.

In [25] a tight end-to-end delay and backlog bound for multi-hop vehicular ad hoc networks which extend the single hop results obtained in [26] are derived. To do that, the authors model the service process offered by the fading channel as a Markov modulated process, with the service rate at each state given by the Shannon capacity limit. The bounds for three scheduling schemes of delay tolerant and delay sensitive arrival flows are then obtained using stochastic network calculus and by utilizing supermartingale inequalities. To enable tractable solutions, the authors consider only homogeneous service curves along a multi-hop path. However, power allocation strategies usually result in a heterogeneous service process along an optimized communication path. Hence, the homogeneity assumption in addition to the lack of explicit representation of the channel gain distribution (or equivalently the SNR at the receiver) for a given allocated transmit power of the wireless link, make the mentioned approach not suitable for power optimization solutions.

Moreover, a version of the deterministic network calculus developed to analyze the performance of wireless sensor networks is the sensor network calculus [27]. This mathematical framework analyses networks represented as sink

trees. The SensorNC provides concepts for in-network processing, called scaling elements. Although this network calculus version can be widely applied, e.g. for sink and node placement strategies, power management in video sensor networks [28] or energy-efficient trajectories for mobile sinks under delay guarantees [29], it lacks a more precise representation of the fading channel and therefore prohibits direct correlation between the service characterization and the transmit power, disabling transmit power adjustment under end-to-end statistical delay constraints.

However, a recently developed theoretical framework has enabled a new analytical toolset for performance analysis of wireless multi-hop fading channels [7]. By means of  $(\min, \times)$ -calculus, bounds on the delay and the backlog are expressed in terms of fading channel gain distribution, working directly in the so called SNR domain. In this domain, multi-hop descriptions of fading channels become mathematically tractable. Based on this work, we have made first attempts to determine the minimal required SNR on a single link in order to meet pre-defined statistical delay requirements [30]. However, [7] addresses only independent and identically distributed (i.i.d.) wireless channel gains, which limits the applicability of the results to general scenarios.

### 1.3. Contributions and Paper Organization

This paper builds on the power minimization algorithm that we proposed in [30] and extends it to multi-hop buffered wireless links with heterogeneously distributed channel gains. Motivated by the discussion above, and the need for energy-efficient heterogeneous multi-hop wireless networks for future industrial applications, we present in this paper the following main contributions:

- Based on the previously derived closed-form expression for the end-to-end statistical delay bound for a multi-hop path consisting of independent, but heterogeneously distributed channel gains, presented in [8], an iterative bound-based power-minimization algorithm for wireless multi-hop heterogeneous networks is developed. We present two variations of the algorithm: (i) minimizing the total transmit power along the path, and (ii) maximizing the network lifetime. A numerical evaluation of the performance of the two variants is performed.
- A proof for the convexity of the delay bound is provided and an evaluation of the bound-based power minimization compared to simulation-based power optimization, i.e., using the exact delay process instead of a delay bound, is presented.

We conduct our analysis and evaluation using two different channel capacity models, (i) an ‘ideal’ Shannon-capacity-based model, and (ii) a more realistic WirelessHART (IEEE 802.15.4e)-based link model. The results that we obtained for power gain (using Shannon-based capacity) and network lifetime extension (assuming an IEEE 802.15.4e-based link capacity) offer significant insights into multi-hop network design, considering heterogeneity of both channel gain as well as battery charge state (i.e., initial energy level).

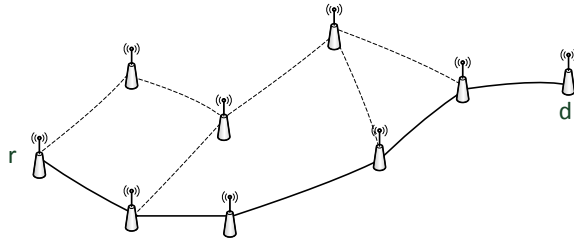


Figure 1: Illustration of the system model

The remaining paper is organized as follows: Section 2 presents the system model and the problem statement. In Section 3 we present the closed-form of the end-to-end delay bound for heterogeneous wireless networks. These results are the basis for the power minimization algorithms presented in Section 4. We discuss the numerical evaluation of the algorithms in Section 5. Finally, Section 6 concludes the paper.

## 2. System Model and Problem Statement

We consider the communication between a source node  $r$  and a destination node  $d$  within a multi-hop wireless network (see Fig. 1). Let the multi-hop path in question, illustrated with solid lines in Fig. 1, be given with an ordered set of buffered links, i.e.,  $\mathbb{L} = \{1, \dots, N\}$ , where  $N$  is the number of links constituting path  $\mathbb{L}$ . We assume a time-slotted system where every link is assigned a time slot of fixed length  $T$ . The nodes propagate the packets originating at node  $r$  along the path every time they are allocated a transmission time slot, according to a given scheduling algorithm. As soon as a packet reaches the destination node, it is passed to its application layer without any additional delay.

Each wireless link  $j \in \mathbb{L}$  is assumed to be a block-fading channel with an average channel gain  $|\bar{h}_j^2|$ . This means, the random instantaneous channel gain  $h_{i,j}^2$  of link  $j$  at time slot  $i$  remains constant within the time interval  $T$ , but varies independently from slot to slot. This assumption is valid for a low mobility environment where the channel gain remains constant within one transmission interval. Furthermore, the frequency-hopping wireless technology is one example where the channel gain varies independently from one transmission interval to the other [31]. Due to the assumptions as block-fading and frequency-hopping, different links are assumed to have statistically independent channel gains while we consider heterogeneously distributed channel gains. Moreover, the instantaneous channel gain consists of two components: the instantaneous random fading component  $h_f^2$  and the constant path-loss  $h_p^2$ , the latter depending on the distance between the nodes and the path-loss exponent, i.e.,  $h_{i,j}^2 = h_{f,i,j}^2 \cdot h_{p,j}^2$ . Although interference is not considered in this paper explicitly, we provide an additional approach, using the concept of *leftover service curve*, to model interference from cross-flows in the network. Together with the transmit power

setting  $p_{i,j}$  and the noise power  $\sigma^2$ , this yields the instantaneous SNR of link  $j$  in time slot  $i$  as:

$$\gamma_{i,j} = \frac{p_{i,j} \cdot h_{i,j}^2}{\sigma^2} \quad (1)$$

Given the instantaneous SNR  $\gamma_{i,j}$ , the resulting service per link  $j$  is given by the link's capacity at time slot  $i$ . We denote the capacity of link  $j$  during time slot  $i$  by the function  $C \cdot \log_2 g(\gamma_{i,j})$ , where  $C$  is the number of symbols that fit within one time slot. The function  $g(\gamma_{i,j})$  defines the instantaneous channel capacity. Hence, by modifying the transmit power we change the channel capacity and therefore, influence the service of the link. Using a Shannon capacity channel model, this function usually takes the form  $g(\gamma_{i,j}) = 1 + \gamma_{i,j}$  or some weighted version of it [32]. We assume that transmitter  $j$  knows only the channel state information for the  $j^{\text{th}}$  channel (corresponding to one of the (up to)  $N$  transmission slots within a transmission frame), but not for the other  $N - 1$  channels. Furthermore, we define  $\vec{\gamma}$  and  $\vec{p}$  as the vectors of average SNRs and transmit power of the links, i.e., nodes along the path, respectively.

At the application layer, we consider a monitoring process generating a measurement value at a regular interval. Therefore, as a model for the arrival flow we consider packets of size  $r_a$  bits arriving per interval  $R_a \cdot T$  with  $R_a \in \mathbb{N}$ . However, the application has strict latency and reliability constraints. These are modeled by the QoS pair  $\{\omega^\varepsilon, \varepsilon\}$  where  $\omega^\varepsilon$  represents a maximum tolerable delay that can be violated at most with probability  $\varepsilon$ . This target delay includes all processing steps below the application layer, therefore including also any queuing delay along the multi-hop path. Since we observe constant data rate arrival, the delay that a packet experiences along the path, depends mainly on the service provided by the links. As discussed above, the service is a random variable, since it depends on the instantaneous capacity, which in turn owns its randomness to the fading present on the link. Hence, random fading is the main source for the delay in the presented system model. Therefore, shaping the links' capacity, i.e., the end-to-end service by smartly adjusting the transmit power on every link will influence the target statistical delay, given as a QoS requirement by the application.

In this paper, we are interested in the trade-off between the energy consumption of the network - mainly driven by the transmit power per node  $p_{i,j}$  - and the resulting delay and delay violation probability. In this context, we are particularly interested in the following two things:

- The minimization of the sum of the transmit power along the path (from now onward referred to as *total transmit power*) under a given QoS pair  $\{\omega^\varepsilon, \varepsilon\}$ , and
- The maximization of the network lifetime given a battery state vector  $\vec{B}$  consisting of battery states per node<sup>1</sup>,  $B_j$ , as well as an energy consumption model, under a given QoS pair  $\{\omega^\varepsilon, \varepsilon\}$ .

---

<sup>1</sup>In this model, node  $j$  refers to the transmitter node preceding link  $j$ .



In the following, we will develop algorithms that determine the corresponding transmit power settings per node under the desired QoS constraints. These algorithms are based on an analytical expression of the network performance (i.e., latency and reliability) in terms of the underlying physical channel properties, which includes the power allocation scheme. Hence, the first step in our efforts is to define the analytical model of the end-to-end delay performance in a wireless multi-hop network in terms of transmit power allocation, which we address in the next section. Then, we develop the two mentioned algorithms in Section 4.

### 3. End-to-End Delay Bound over Heterogeneous Links

In this section, we derive the end-to-end performance bounds based on stochastic network calculus for heterogeneous, multi-hop communication paths. For wireless fading channels, end-to-end probabilistic bounds have only been obtained for concatenated i.i.d. service processes (i.e., for multi-hop wireless links all having independent and identically distributed fading processes) [7]. In order to apply these results to heterogeneous networks, we generalize the available results to arbitrarily distributed random service processes. At this point we stress, that arbitrarily i.e., heterogeneously distributed service processes characterize not only with random channel gains following different distributions, but also with channel gains represented by random variables drawn from the same distribution, however, with different mean values.

For reader's benefit, we first recap some network calculus basics before presenting the theoretical basis for the development of our algorithms.

#### 3.1. Stochastic Network Calculus

Stochastic network calculus considers queuing systems and networks of systems with stochastic arrival and departure processes, where the bivariate functions  $A(\tau, t)$ ,  $D(\tau, t)$  and  $S(\tau, t)$ , for any  $0 \leq \tau \leq t$ , denote the *cumulative* arrivals to the system, departures from the system, and service offered by the system, respectively, in the interval  $[\tau, t)$ . Recall that we consider a discrete time model, where time slots have a duration  $T$  and  $i \geq 0$  denotes the index of the respective time-slot. Hence,  $t, \tau, i \in \mathbb{Z}$ .

A lossless system with service process  $S(\tau, t)$  satisfies the input/output relationship  $D(0, t) \geq A \otimes S(0, t)$ , where  $\otimes$  is the  $(\min, +)$  convolution operator defined as

$$x \otimes y(\tau, t) = \inf_{\tau \leq u \leq t} \{x(\tau, u) + y(u, t)\} . \quad (2)$$

In this approach, we are generally interested in probabilistic bounds of the form  $\Pr [W(t) > w^\varepsilon] \leq \varepsilon$ , which is also known as the *violation probability* for a target delay  $w^\varepsilon$ , under the following system stability condition:

$$\lim_{t \rightarrow \infty} \frac{A(0, t)}{t} < \lim_{t \rightarrow \infty} \frac{S(0, t)}{t} . \quad (3)$$

Modeling wireless links in the context of network calculus however is not a trivial task. A particular difficulty arises when we seek to obtain a stochastic characterization of the cumulative service process of a wireless fading channel, as also witnessed in the context of the effective service capacity of wireless systems [33]. A promising, recent approach for wireless networks has been proposed in [7] where the queuing behavior is analyzed directly in the “domain” of channel variations instead of the bit domain [34, 20, 35, 36, 18, 33]. This can be interpreted as the *SNR domain* (thinking of bits as “SNR demands” that reside in the system until these demands can be met by the channel) and the type of network calculus is called  $(\min, \times)$  calculus.

The cumulative arrival, service, and departure processes in the bit domain, i.e.,  $A$ ,  $D$ , and  $S$ , are related to their SNR domain counterparts (represented in the following by calligraphic capital letters  $\mathcal{A}$ ,  $\mathcal{D}$ , and  $\mathcal{S}$ , respectively) through the exponential function. Thus, we have  $\mathcal{A}(\tau, t) \triangleq e^{A(\tau, t)}$ ,  $\mathcal{D}(\tau, t) \triangleq e^{D(\tau, t)}$  and  $\mathcal{S}(\tau, t) \triangleq e^{S(\tau, t)}$ . Due to the exponential function, these cumulative processes become products of the increments in the bit domain. In the following, we will assume  $\mathcal{A}(\tau, t)$  and  $\mathcal{S}(\tau, t)$  to have stationary and independent increments. We denote them by  $\alpha$  for the arrivals and  $g(\gamma)$  for the service. For instance, assuming a single-hop wireless system with a point-to-point channel, where the channel capacity is expressed through the well-known Shannon capacity, the service increment is defined as follows

$$s_i = \log(g(\gamma_i)) = C \log_2(1 + \gamma_i), \quad (4)$$

where  $s_i$  is the random service in bits offered by the system in time slot  $i$ ,  $C$  is the number of transmitted symbols per time slot and  $\gamma_i$  is the instantaneous SNR. Then, we can obtain the cumulative service in the SNR domain as

$$\mathcal{S}(\tau, t) = \prod_{i=\tau}^{t-1} e^{s_i} = \prod_{i=\tau}^{t-1} g(\gamma_i) = \prod_{i=\tau}^{t-1} (1 + \gamma_i)^C, \quad (5)$$

where  $\mathcal{C} = C/\log 2$ . Furthermore, in case of first-come first-served order, the delay at time  $t$  is obtained as follows

$$W(t) = \mathcal{W}(t) = \inf\{i \geq 0 : \mathcal{A}(0, t)/\mathcal{D}(0, t+i) \leq 1\}. \quad (6)$$

An upper bound  $\varepsilon$  for the delay violation probability  $\Pr[W(t) > w^\varepsilon]$  can be derived based on a transform of the cumulative arrival and service processes in the SNR domain using the moment bound. In [7] it was shown that such a violation probability bound for a given  $w^\varepsilon$  can be obtained as  $\inf_{s>0} \{\mathcal{K}(s, t + w^\varepsilon, t)\}$ .

We refer to the function  $\mathcal{K}(s, \tau, t)$  as the *kernel* defined as

$$\mathcal{K}(s, \tau, t) = \sum_{i=0}^{\min(\tau, t)} \mathcal{M}_{\mathcal{A}}(1 + s, i, t) \mathcal{M}_{\mathcal{S}}(1 - s, i, \tau), \quad (7)$$

where the function  $\mathcal{M}_{\mathcal{X}}(s)$  is the Mellin transform [37] of a random process, defined as

$$\mathcal{M}_{\mathcal{X}}(s, \tau, t) = \mathcal{M}_{\mathcal{X}(\tau, t)}(s) = \mathbb{E}[\mathcal{X}^{s-1}(\tau, t)], \quad (8)$$

for any  $s \in \mathbb{C}$ , whenever the expectation exists. We restrict our derivations in this work to real valued<sup>2</sup>  $s \in \mathbb{R}$ . Introducing the Mellin transform in the performance analysis of wireless fading channels results into tractable mathematical expressions when computing network calculus bounds, which in turn results in scalable closed-form solutions. The motivation for the usage of Mellin transforms comes from their property to allow analytical solutions for the quotients or products of random variables. These quotients and products represent the performance bounds in the  $(\min, \times)$  calculus. Although our results base on the Mellin transforms, due to their neat properties when working with fading channels, we stress that the MGF-based network calculus presented in [18] can also be used for performance analysis of wireless fading channels. However, the form that the end-to-end delay bound, presented below, takes using Mellin transforms, is more convenient to work with, when analyzing multi-hop networks. Using the assumption of stationary increments of the arrival and service processes, their Mellin transforms become independent of the time instance, and hence we write  $\mathcal{M}_{\mathcal{X}}(s, t - \tau)$ . In addition, as we only consider stable queuing systems in steady-state, the kernel becomes independent of the time instance  $t$  and we denote  $\mathcal{K}(s, t + w^\varepsilon, t) \stackrel{t \rightarrow \infty}{=} \mathcal{K}(s, -w^\varepsilon)$ .

The strength of the Mellin-transform-based approach becomes apparent when considering block-fading channels. The Mellin transform for the cumulative service process in the SNR domain is given by

$$\mathcal{M}_{\mathcal{S}}(s, \tau, t) = \prod_{i=\tau}^{t-1} \mathcal{M}_{g(\gamma)}(s) = \mathcal{M}_{g(\gamma)}^{t-\tau}(s) = \mathcal{M}_{\mathcal{S}}(s, t - \tau), \quad (9)$$

where  $\mathcal{M}_{g(\gamma)}(s)$  is the Mellin transform of the stationary and independent service increment  $g(\gamma)$  in the SNR domain. The second step in Eq. (9) is possible due to the mutual independence of the service processes, which in turn, is guaranteed by the assumption on block-fading channels and the frequency-hopping scheme. The function  $g(\cdot)$  is associated with the channel capacity of a point-to-point fading channel as defined by Eq. (4). However, it can also model more complex system characteristics, most importantly scheduling effects. It is important here to note that,  $g(\cdot)$  can represent *any* service capacity, as long as it is being represented in the SNR domain. In this work we focus, however, on wireless fading channels.

Assuming the cumulative arrival process in the SNR domain to have stationary and independent increments, we denote the corresponding Mellin transform by  $\mathcal{M}_{\mathcal{A}}(s, t - \tau) = \prod_{i=\tau}^{t-1} \mathcal{M}_{\alpha}(s) = \mathcal{M}_{\alpha}^{t-\tau}(s)$ . Substituting these two cumulative processes in Eq. (7), for the general form of the steady-state kernel for a

---

<sup>2</sup>We note that by definition of  $\mathcal{X}(\tau, t) = e^{X(\tau, t)}$ , the Mellin transform  $\mathcal{M}_{\mathcal{X}}(s, \tau, t) = \mathbb{E}[e^{(s-1)X(\tau, t)}]$  after substitution of parameter  $s = \theta + 1$  implies also a solution for the moment-generating function (MGF), that is the basis of the effective capacity model [33] and of an MGF network calculus [18].

communication channel we get

$$\mathcal{K}(s, -w) = \frac{\mathcal{M}_{g(\gamma)}^w(1-s)}{1 - \mathcal{M}_\alpha(1+s)\mathcal{M}_{g(\gamma)}(1-s)} \quad (10)$$

for any  $s > 0$ , for which the expectation defined in Eq. (8) exists and whenever the following stability condition holds,

$$\mathcal{M}_\alpha(1+s)\mathcal{M}_{g(\gamma)}(1-s) < 1. \quad (11)$$

The minimal value of Eq. (10) over all  $s > 0$ , i.e.,  $\inf_{s>0}\{\mathcal{K}(s, -w)\}$ , represents the bound on the delay violation probability for a given target delay  $w$ . Shaping any of the  $\mathcal{M}_\alpha$  or  $\mathcal{M}_{g(\gamma)}$  or in other words shaping the arrival to and/or the service of the communication channel, allows manipulation of the kernel, s.t. for a given target delay violation probability  $\varepsilon$ ,  $\inf_{s>0}\{\mathcal{K}(s, -w)\} \leq \varepsilon$ . In this work, we aim towards meeting the statistical delay constraints by changing the service of the wireless channel by adjusting its SNR, i.e., transmit power of the node.

An asymptotic lower bound, which coincides with the upper bound when  $w \rightarrow \infty$ , can be obtained using the large-deviation theory [7].

### 3.2. Recursive Formula for the End-to-End Delay Bound

A further advantage of network calculus is the ability to capture a cascade of service processes into a joint service curve using the server concatenation theory. This property is especially useful for performance analysis of multi-hop networks. Similar to the  $(\min, +)$  algebra, the joint service curve is obtained through the end-to-end convolution according to the  $(\min, \times)$  network calculus. For a path  $\mathbb{L}$ , consisting of links with random service processes  $S_j, j \in \{1, \dots, N\}$ , it is defined as follows:

$$\mathcal{S}^{\mathbb{L}}(\tau, t) = \mathcal{S}_1 \otimes \mathcal{S}_2 \otimes \dots \otimes \mathcal{S}_N(\tau, t), \quad (12)$$

where  $\mathcal{S}_1 \otimes \mathcal{S}_2(\tau, t) = \inf_{\tau \leq i \leq t} \{\mathcal{S}_1(\tau, i) \cdot \mathcal{S}_2(i, t)\}$ .

A Mellin transform of the  $(\min, \times)$  convolution is not available. Instead, we define a bound on the Mellin transform of the end-to-end service based on the server concatenation defined above and using the union bound<sup>3</sup>, also known as Boole's inequality.

Let  $\mathcal{S}_1(\tau, t)$  and  $\mathcal{S}_2(\tau, t)$  be two independent non-negative bivariate random processes representing the service processes of link 1 and 2, respectively. For  $s < 1$ , the Mellin transform of the  $(\min, \times)$  convolution of  $\mathcal{S}_1$  and  $\mathcal{S}_2$ , denoted by  $\mathcal{S}_1 \otimes \mathcal{S}_2(\tau, t)$ , is bounded by

$$\mathcal{M}_{\mathcal{S}_1 \otimes \mathcal{S}_2}(s, \tau, t) \leq \sum_{i=\tau}^t \mathcal{M}_{\mathcal{S}_1}(s, \tau, i) \cdot \mathcal{M}_{\mathcal{S}_2}(s, i, t) \quad (13)$$

---

<sup>3</sup>Note that in case of dependent random variables, i.e., service processes, the bound can be derived using the Hölder's inequality [7].

Note that in Eq. (13) the union bound is applied in order to obtain an analytical expression of the joint service curve of two random service processes. This analytical representation has to be “paid” with a rather loose bound on the actual joint service curve. A sharper stochastic bound on the delay distribution can be obtained by using so called service-martingales [26]. However, this approach has not been extended to multi-hop networks up to date.

Hence, the corresponding Mellin transform of path  $\mathbb{L}$  can be bounded by [7]:

$$\begin{aligned} \mathcal{M}_{\mathcal{S}^{\mathbb{L}}}(s, \tau, t) &\leq \sum_{i_1=i_0}^t \sum_{i_2=i_1}^t \dots \sum_{i_{N-1}=i_{N-2}}^t \mathcal{M}_{\mathcal{S}_1}(i_1 - i_0) \cdot \mathcal{M}_{\mathcal{S}_2}(i_2 - i_1) \dots \mathcal{M}_{\mathcal{S}_N}(i_N - i_{N-1}) \\ &= \sum_{i_1 \dots i_{N-1}}^t \prod_{j=1}^N \mathcal{M}_{\mathcal{S}_j}^{i_j - i_{j-1}}(s), \end{aligned} \quad (14)$$

with  $\tau = i_0 \leq i_1 \leq \dots \leq i_N = t$ . Notice that  $\mathcal{M}_{\mathcal{S}_j}(s)$  denotes the Mellin transform of the (stationary) SNR service increments of link  $j$ .

As one may notice from Eq. (13), this results in a cumbersome computation, especially for links having different channel gain distribution, since  $N$  convolution processes have to be computed, each of them depending on  $t$ . A significant simplification of Eq. (13), representing a mathematically easier-to-grasp analytical solution was presented in our previous work [8]. The derived formula for the delay bound avoids the tedious task of performing  $N$  nested sums in Eq. (14). Hence, we define  $\mathcal{K}^{\mathbb{L}}$  as the kernel for a path  $\mathbb{L}$  containing  $N$  links, similar to Eq. (7), where we replace  $\mathcal{M}_{\mathcal{S}}(1-s, i, \tau)$  with  $\mathcal{M}_{\mathcal{S}^{\mathbb{L}}}(1-s, i, \tau)$  for  $\mathcal{S}^{\mathbb{L}}$  defined in Eq. (12). Once that Mellin transform can be determined, a probabilistic end-to-end delay bound for path  $\mathbb{L}$  can be computed using Eq. (7) that satisfies the following inequality [7]:

$$\inf_{s \geq 0} \{ \mathcal{K}^{\mathbb{L}}(s, -w^\varepsilon) \} \leq \varepsilon. \quad (15)$$

Let  $m$  and  $N$  refer to the  $m^{\text{th}}$  and  $N^{\text{th}}$  link of path  $\mathbb{L}$ , respectively. For a given path  $\mathbb{L} \setminus \{N\}$  of links with independent and heterogeneously distributed service processes, with kernel  $\mathcal{K}^{\mathbb{L} \setminus \{N\}}$ , the  $\mathcal{K}^{\mathbb{L}}$  can be obtained in terms of  $\mathcal{K}^{\mathbb{L} \setminus \{N\}}$  as follows

$$\begin{aligned} \mathcal{K}^{\mathbb{L}}(s, -w) &= \frac{\mathcal{M}_{g(\gamma_N)}(1-s)}{\mathcal{M}_{g(\gamma_N)}(1-s) - \mathcal{M}_{g(\gamma_m)}(1-s)} \mathcal{K}^{\mathbb{L} \setminus \{m\}}(s, -w) \\ &\quad + \frac{\mathcal{M}_{g(\gamma_m)}(1-s)}{\mathcal{M}_{g(\gamma_m)}(1-s) - \mathcal{M}_{g(\gamma_N)}(1-s)} \mathcal{K}^{\mathbb{L} \setminus \{N\}}(s, -w) \end{aligned} \quad (16)$$

for any  $m \in \{1, 2, \dots, N-1\}$ . The proof of the closed-form solution for the end-to-end delay bound given with Eq. (16) can be found in [8].

A direct consequence of Eq. (16) and Eq. (15) is that the delay bound for path  $\mathbb{L}$  can be obtained from recursively computing the kernel according to the

theorem. In this recursion, the number of summands increases with the number of hops. For an  $N$ -hop path there are  $2^{N-1}$  summands, as each geometric sum results into two summands. Furthermore, the stability condition in Eq. (11) needs to hold for every individual link  $j \in \{1, \dots, N\}$ , i.e.,:

$$\max_j (\mathcal{M}_\alpha (1 + s) \cdot \mathcal{M}_{g(\gamma_j)} (1 - s)) < 1$$

has to be fulfilled. Note that the links  $m$  and  $N$  have to be chosen in such way, such that their average SNRs are not equal, avoiding the denominator  $\mathcal{M}_{g(\gamma_m)} (1 - s) - \mathcal{M}_{g(\gamma_N)} (1 - s)$  to be equal to 0. In case several links along the path characterize with equal average SNR, the joint service curve of these sub-paths with homogeneously distributed channel gains can be computed using the following equation [7]:

$$\mathcal{M}_{\mathcal{S}_{\text{hom}}}(s, \tau, t) \leq \binom{N - 1 + t - \tau}{t - \tau} \cdot (\mathcal{M}_{g(\gamma)}(s))^{t - \tau}$$

Finally, note in particular that in principle Eq. (16) can be generalized to any link  $j$  and the path  $\mathbb{L} \setminus \{j\}$ . This allows an efficient recomputation of the kernel in case that any of the links of the path change their primary distribution, for instance due to a changed propagation environment. In contrast, in case of using Eq. (14), if a single link changes its distribution, a complete recomputation of the joint service curve characterization has to be performed, which is significantly more complex.

We show next that the kernel described by Eq. (16) is convex in  $s > 0$ . The following theorem states this convexity.

**Theorem 1.** *The steady-state kernel  $\mathcal{K}(s, -w)$  for a communication channel,*

$$\mathcal{K}(s, -w) = \frac{\mathcal{M}_{g(\gamma)}^w (1 - s)}{1 - \mathcal{M}_\alpha (1 + s) \mathcal{M}_{g(\gamma)} (1 - s)},$$

*is convex in  $s, \forall s > 0$  for which the stability condition  $\mathcal{M}_\alpha (1 + s) \mathcal{M}_{g(\gamma)} (1 - s) < 1$  holds. Furthermore, the end-to-end kernel  $\mathcal{K}^{\mathbb{L}}(s, -w)$  for a multi-hop path  $\mathbb{L}$  is convex in  $s$ , for every  $s$  within the stability interval.*

The proof of Theorem 1 is given in Appendix B.

The convexity of the kernel confirms the existence of a unique optimum and motivates us to specify bound-based algorithms for optimization, i.e., transmit power allocation along the path which reaches the optimum. These are presented in Section 4.

What is particularly important about the presented results is that, both Eq. (16) and Theorem 1 hold for *any* kernel for a communication channel, whose service is defined in the SNR domain. In this paper, however, we focus our analysis on wireless fading channels and two kernel types - namely the ones specified for a Shannon- and a WirelessHART-based service.

### 3.3. Heterogeneous Path with Cross-Traffic

The proof of Eq. (16), given in the appendix, shows that the recursion obtained for the end-to-end delay bound results from the recursion in the Mellin transform of the joint service curve. As a result, the stepwise construction of a multi-hop path's service curve will further simplify the computation of other elements in  $(\min, \times)$  network calculus, such as the delay bound. We demonstrate this by providing the leftover service curve for the considered path when cross-traffic is present, i.e., additional flows other than  $A(\tau, t)$  are sharing the intermediate links in the path that the through-flow traverses. Let the SNR arrival processes of the cross-traffic at each intermediate link be i.i.d. and denoted by  $\mathcal{A}_c(\tau, t) = e^{k_c(t-\tau)}$ , where we assume a constant arrival rate of  $k_c$  bits per time slot. Assume further that the arrivals from the original through-flow and the cross-traffic as well as the service processes at each link are independent. We can then compute a bound on the Mellin transform of the end-to-end service process offered to the through-flow, i.e., the *leftover service curve* using the following result:

**Theorem 2.** *Consider a flow traversing a cascade of wireless fading channels. The service at each node is shared by the through-flow and an independent cross-flow characterized by the SNR arrival process  $\mathcal{A}_c(\tau, t)$ . Let  $\mathcal{S}_c^{\mathbb{L}}(\tau, t)$  denote the end-to-end leftover service provided to the through-flow. Then,  $\forall s < 1$ ,*

$$\begin{aligned} \mathcal{M}_{\mathcal{S}_c^{\mathbb{L}}}(s, \tau, t) \leq & \left( \frac{\mathcal{M}_{g(\gamma_N)}(s)}{\mathcal{M}_{g(\gamma_N)}(s) - \mathcal{M}_{g(\gamma_m)}(s)} \cdot \mathcal{M}_{\mathcal{S}_c^{\mathbb{L} \setminus \{m\}}}(s, \tau, t) \right) \\ & + \left( \frac{\mathcal{M}_{g(\gamma_m)}(s)}{\mathcal{M}_{g(\gamma_m)}(s) - \mathcal{M}_{g(\gamma_N)}(s)} \cdot \mathcal{M}_{\mathcal{S}_c^{\mathbb{L} \setminus \{N\}}}(s, \tau, t) \right), \end{aligned} \quad (17)$$

for any  $m \in \{1, 2, \dots, N-1\}$  and  $\mathcal{M}_{\mathcal{S}_c^{\{1\}}}(s, \tau, t) = (e^{k_c(1-s)} \cdot \mathcal{M}_{g(\gamma_1)}(s))^{t-\tau}$ .

**Proof 1.** According to Lemma 1 in [7] we obtain the Mellin transform of the leftover service curve for a single channel:

$$\begin{aligned} \mathcal{M}_{\mathcal{S}_c^{\{1\}}}(s, \tau, t) &= \mathcal{M}_{s/\mathcal{A}_c}(s, \tau, t) \\ &= \mathcal{M}_{g(\gamma_1)}(s, \tau, t) \cdot \mathcal{M}_{\mathcal{A}_c}(2-s, \tau, t) \\ &\leq \left( e^{k_c(1-s)} \cdot \mathcal{M}_{g(\gamma_1)}(s) \right)^{t-\tau}, \end{aligned} \quad (18)$$

since the Mellin transform of a quotient of two independent random variables  $X$  and  $Y$  is given by  $\mathcal{M}_{X/Y}(s) = \mathbb{E}[X^{s-1}] \mathbb{E}[Y^{1-s}] = \mathcal{M}_X(s) \cdot \mathcal{M}_Y(2-s)$ .

Substituting  $e^{k_c(1-s)} \mathcal{M}_{g(\gamma_N)}(s)$  for  $\mathcal{M}_{g(\gamma_N)}$  in the joint service curve derivation, the expression given by Eq. (17) follows by applying the recursion to the leftover service curve of path  $\mathbb{L}$ ,  $\mathcal{M}_{\mathcal{S}_c^{\mathbb{L}}}(s, \tau, t)$ .

#### 4. Bound-Based Power Minimization Algorithms

As already mentioned, an essential aspect of industrial wireless networks, besides the importance of QoS-awareness, is their energy-efficient operation. Especially for battery-powered network devices, often attached to machines in order to control them or measure their functional status, it is important to prolong network partitioning time by extending nodes' battery lifetime. Since the radio chip is usually one of the largest consumers of energy in low-power networks [38], one way of providing energy efficiency is to minimize the transmit power, as one of the easily modifiable parameters in wireless transceivers. In addition, minimizing transmit power not only increases energy savings, but also reduces potential interference to neighboring transmissions. In a multi-hop setting, power optimization mainly needs to take two issues into account. On the one hand, heterogeneous link statistics can be exploited to reduce power consumption.

On the other hand, heterogeneous battery states (i.e., energy levels) affect the transmit power setting. Thus, in this section we develop and present algorithms that take these effects into account in order to minimize transmit power or maximize network lifetime under statistical end-to-end constraints as represented by the above presented bound. The proposed algorithms are run on a central node in the network, which is provided with a constant power supply and enough computing power, so that their performance is not jeopardized. This node contains all necessary information to run the algorithms, such as the target QoS requirements by the application, the size of incoming packets and the average channel gain information of all links in the network. The algorithm is executed offline, as soon as the channel statistics was collected using control packets and prior application data has been sent. In order to be able to provide well-timed reaction to environment and QoS requirements changes, the algorithm can be executed in specific time intervals during network operation as well.

##### 4.1. Transmit Power Minimization Algorithm

We initially raise the following question: What is the optimal average SNR, i.e., minimal sum transmit power needed on all links along a path to meet a target end-to-end delay  $w^\varepsilon$  with probability  $1 - \varepsilon$ ? This question is difficult to answer, as for the violation probability  $\varepsilon$  no accurate analytical model exists (to date) that can relate it precisely to the average SNRs. The only option is to resort to system simulations to determine the corresponding SNRs. In contrast, we propose to base system optimization on the multi-hop delay bound, as presented in Eq. (16). Hence, we are interested in the solution of the following



optimization problem for a given multi-hop path  $\mathbb{L} = \{1, \dots, N\}$ :

$$\begin{aligned} \min \quad & \sum_{j=1}^N p_j, \\ \text{s. t.} \quad & \inf_{s>0} \{\mathcal{K}^{\mathbb{L}}(s, -w^\varepsilon)\} \leq \varepsilon \\ & \max_j (\mathcal{M}_\alpha (1+s) \cdot \mathcal{M}_{g(\gamma_j)} (1-s)) < 1. \end{aligned}$$

Due to the complexity of the kernel function and the stability condition, no analytical solution for the bound-based optimal SNRs can be derived (see e.g. the complex forms of the kernel for Rayleigh-fading wireless channel (Eq. (20)) and for a WirelessHART system (Eq. (22)) from Section 5.1.1 and Section 5.2.1, respectively). Instead, we propose a binary search algorithm in two dimensions (along  $s > 0$  and along the SNRs) to solve the given minimization problem (see Algorithm 2 in Appendix A). Notice that minimizing  $\bar{\gamma}_j$  leads to minimization of the transmit power per hop, since  $\bar{\gamma}_j = p_j \cdot |\bar{h}_j^2| / \sigma^2$ .

As already stated in Theorem 1, the kernel described by Eq. (16) is convex in  $s$  for  $\forall s \in (0, b)$ , where  $b$  is the last point for which the stability condition in Eq. (11) holds. Further, for  $\forall s \in (0, b)$  the Mellin transform, defined as in Eq. (8), exists. From this it follows that the proposed algorithm results in a global bound-based minimum. Figure 2 illustrates the kernel of several links with different average SNR, where the instantaneous channel capacity is given by Eq. (4). The figure shows that the delay bound function of a single link  $\mathcal{K}(s, -w)$  is convex in  $s$  and monotone in  $\bar{\gamma}$ . For the computation of the kernel in the figure, we assumed a block-fading wireless link with constant arrival rate and random service increments that are characterized by the Shannon capacity. We further notice that, as the SNR either increases or decreases, the optimal  $s^*$  (which minimizes the delay bound function) moves to the right or to the left, respectively.

For any given transmit power vector  $\vec{p} = \{p_1, \dots, p_N\}$  and resulting fixed SNR vector  $\vec{\gamma} = \{\bar{\gamma}_1, \dots, \bar{\gamma}_N\}$ , the value  $s^*$  for which  $\mathcal{K}^{\mathbb{L}}(s, -w)$  is minimal, is determined by performing a binary search along the interval  $(0, b)$ . The main idea here is to cut the interval  $(0, b)$  into four areas through fixing five points (see Fig. 3), where  $s_m$  is the middle point of  $(0, b)$ . Based on this partition, the algorithm traces the gradients and splits the range where the minimum of  $\mathcal{K}^{\mathbb{L}}(s, -w)$  is located. The function is called recursively until the smallest size of an interval has been reached, defined with the input parameter  $\Delta_{\min}$ . At this point, the middle point  $s_m$  of the last considered partition is returned as  $s^*$ , i.e., as the point  $s$  for which  $\mathcal{K}^{\mathbb{L}}(s, -w)$  reaches its minimum. The pseudo code for the binary search of  $s^*$  is given in Algorithm 1 in Appendix A.

For the search in the second dimension along the  $\bar{\gamma}$  dimension (see Algorithm 2 in Appendix A), we start by allocating a predefined maximal transmit power  $p_{\max}$  to each node along the path. In each iteration, the gradient of the end-to-end kernel  $\mathcal{K}^{\mathbb{L}}(s^*, -w)$  is computed for every link on the path, i.e.,  $\forall j \in \{1, \dots, N\}$ . The smallest gradient defines the link  $j$  whose transmit power is

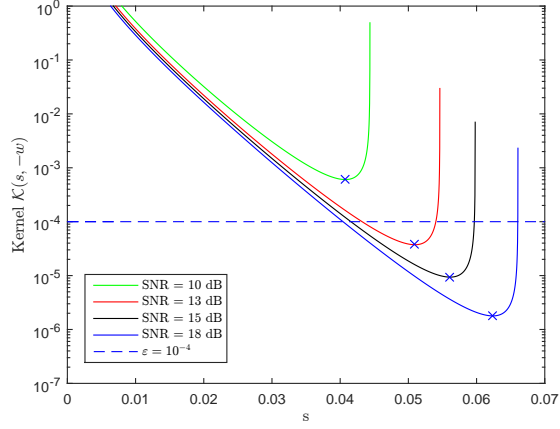


Figure 2: The delay bound function  $\mathcal{K}(s, -w)$  is convex in  $s$ . It is obtained for  $r_a = 50$  bits per time slot and target delay  $w = 5$  time slots. Its minimum is marked with a cross and shifts to the right as the average SNR on the link is increased. The target delay violation probability  $\varepsilon$  is presented with a dotted line.

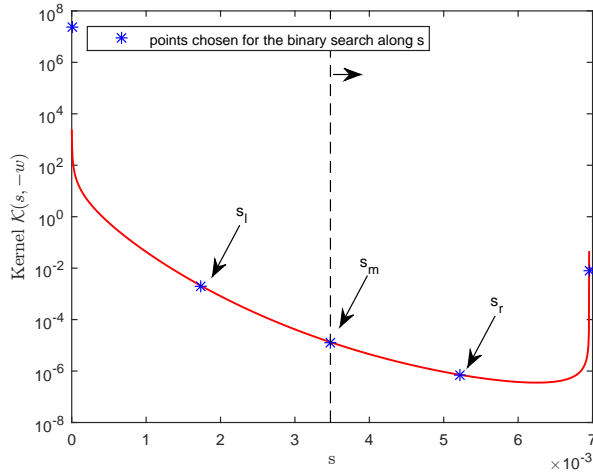


Figure 3: The chosen points within the interval  $(0, b)$  for the binary search along dimension  $s$ .  $s_l$  and  $s_r$  mark the middle of the left and right half of the interval, respectively, while  $s_{\text{start}}$  and  $s_{\text{end}}$  represent 0 and  $b$ , respectively.

going to be changed in that iteration.  $\vec{\gamma}_j$  is the vector of average SNRs per link in which the  $j$ -th SNR is replaced by the SNR obtained when  $p_j$  is decreased for some predefined  $\Delta p$  (line 11 in Algorithm 2, Appendix A). In each iteration a new kernel is computed (denoted with  $\hat{\varepsilon}$ ). In case the newly computed kernel is bigger than the target violation probability  $\varepsilon$ ,  $\Delta p$  is halved, so that a further decrease of the transmit power is possible.  $p_j$  is halved until it reaches a predefined minimal value  $\Delta p_{\min}$ . Although this approach results into smaller decreasing (or increasing) steps of the transmit power, it enables better proximity of the final kernel to the target delay violation probability, i.e., it leads to higher precision of the quasi-optimal solution. Since the power minimization algorithm is meant to be executed on a central node equipped with a high performance CPU, the running time of the algorithm and its performance optimization is out of the scope in this work. We rather concentrate on the correctness of the achieved solution. Hence, we trade the performance of the power minimization algorithm (expressed in total number of iterations needed to reach an optimal solution) in order to obtain higher optimization success, i.e., obtain an almost-optimal solution, as close as possible to the actual optimum.

The algorithm returns the current vector  $\vec{p}$  as the optimal one, either when all links are assigned with the minimal possible transmit power or the smallest possible  $\Delta p$  has been reached and the transmit power along the links cannot be further reduced. It may happen though, that the target delay cannot be met. In this case, the returned optimal transmit power vector equals  $\vec{p} = \vec{p}_{\max}$ . In the optimal case the algorithm exits when the obtained kernel has approached the target violation probability very close from below, i.e.,  $\hat{\varepsilon} \in [\varepsilon - \Delta_\varepsilon, \varepsilon]$  for some predefined  $\Delta_\varepsilon$ .

The obtained bound-based solution for  $\vec{\gamma}$  and  $\vec{p}$  is quasi-optimal, since the binary-search algorithm approaches to the optimal  $s^*$  and the target  $\varepsilon$ . Nevertheless, the input parameters  $\Delta_\varepsilon$ ,  $\Delta p_{\min}$  and  $p_{\max}$  can be used to make a trade-off between the algorithm's precision and its performance, i.e., the needed number of iterations to reach the quasi-optimal solution.

#### 4.2. Network Lifetime Maximization Algorithm

For industrial automation applications, reducing the transmit power results into lower interference with neighbouring networks, which leads to better coexistence of multiple wireless technologies within the same area. Furthermore, it increases the energy-efficiency of the wireless network, which is crucial for applications where battery-powered devices are used. Early battery exhaustion will cause a shorter overall network lifetime as well as a potential premature network partitioning. Therefore, extending battery lifetime is another important aspect in the performance analysis of industrial wireless applications.

In applications where network lifetime is more important than pure energy saving, the bound-based power-minimization algorithm defined in the previous section may not be ideal. It is worth noting that in the case of heterogeneous multi-hop networks, the proposed algorithm may result in an unequal depletion of the battery energy levels at different hops, which may result in shorter network lifetime. An alternative approach is to allow nodes with lower energy levels to

use lower transmit power, which may result in an increased delay, while other nodes pick-up the slack by increasing their transmit power to compensate for the extra delay introduced by that node. We therefore propose a separate algorithm for network lifetime maximization, which is a modification of the bound-based power-minimization algorithm defined in the previous section.

In this work, we assume a network (or a path) is no longer useful when any of the nodes' battery is fully depleted. Nevertheless, the algorithm can also be used, with few modifications, to handle more resilient wireless networks design. The difference from the previous algorithm is mainly related to the decision regarding whose link's transmit power to decrease in each subsequent iteration of the algorithm. In the new algorithm, it is redefined into choosing the transmitter that has the least charged battery at that moment of time. For this purpose we look at the battery full states (denoted by the vector  $\vec{B}$ ) of the nodes along the path  $\mathbb{L}$ . The goal is to maximize the minimal battery lifetime or duration of battery operation  $\theta_j, j \in \{1, \dots, N\}$ , among all batteries (the vector of battery durations is denoted by  $\vec{\theta}$ ). Each relay node can be in one of the following states: idle, send and receive. In this work we don't differentiate between an idle and sleep state and consider both of them as idle state. The battery consumption during the idle and the receive phase is dependent on the transceiver, while the energy consumption in the sending state is mainly dictated by the transmit power. Notice further, that the source node cannot be in receive mode, while the destination does not send packets and is therefore excluded from the decision process. Having a time slotted system with slot length  $T$ , the rest of the time slot assigned to a node, in which it neither sends nor receives the packet, is spent in an idle state.<sup>4</sup>

To handle the effect described above, we formulate the following bound-based network lifetime maximization problem:

$$\begin{aligned} & \max_{j=1\dots N} \min \{\theta_j\}, \theta_j = \frac{B_j}{p_j \cdot T} \\ \text{s.t.} \quad & \inf_{s>0} \{\mathcal{K}^{\mathbb{L}}(s, -w^\varepsilon)\} \leq \varepsilon \\ & \max_j (\mathcal{M}_\alpha (1 + s) \cdot \mathcal{M}_{g(\gamma_j)} (1 - s)) < 1. \end{aligned}$$

In comparison to the transmit power minimization algorithm presented in Sec. 4.1, the network lifetime maximization algorithm selects the node with the minimal battery duration as a candidate whose transmit power will be reduced in that iteration. The assigned transmit power can be selected in the interval  $(p_{\min}, p_{\max})$ , both depending on the chosen hardware. Similar to the gradient-based algorithm, the transmit power is reduced in steps of  $\Delta p$  until the resulting

---

<sup>4</sup>Even if the proposed battery model is rather simplistic, it is a widely used model for evaluating the communication-related energy consumption behaviour in wireless sensor networks [39, 40]. Other radio states such as preparing the transmitter and the receiver to send and receive data, respectively, or switching between Tx and Rx state, will proportionally scale the power consumption per time slot and won't add any significant insight to our analysis.

delay bound function (computed using Eq. (16)) is bigger than the target one. Each time this is the case,  $\Delta p$  is halved until some predefined  $\Delta p_{\min}$  has been reached. The pseudo-code of the network lifetime algorithm is given in Algorithm 3 in Appendix A. Among the above mentioned parameters, the QoS requirements  $w$  and  $\varepsilon$ , together with the payload size  $r_a$  and the maximal frame size  $k_a$ , that can be sent per time slot on the channel, are input parameters to the algorithm.

## 5. Numerical Evaluation

In this section, we present numerical evaluations of the power minimization algorithms based on the end-to-end delay bound over heterogeneous links. In the following subsections we then focus on the power minimization algorithms. In Sec. 5.1 we evaluate our suggested algorithm for various path compositions. In Sec. 5.2 we present results that correspond to network's lifetime maximization, considering a more realistic transceiver node model in a WirelessHART network based on the IEEE 802.15.4 standard [41]. All presented results rely on Eq. (16), which was validated via simulations. In [8] we show that the provided closed-form solution for the end-to-end delay bound is indeed an upper bound of the simulated delay violation probability for various multi-hop scenarios, observing a gap of approximately one order of magnitude. It is important to note that, the decay rate of the computed delay violation probability is exactly the same as the one obtained via simulations, which suggests that the bound is asymptotically tight. We refer the interested reader to [8] for a detailed description of the validation.

### 5.1. Evaluation of the Power-Minimization Algorithm

We now turn to the evaluation of the bound-based transmit power minimization algorithm presented in Section 4.1. Recall that the algorithm minimizes the total transmit power over all links of a multi-hop path based on the analytically determined end-to-end kernel according to Eq. (16). The target end-to-end delay violation probability  $\varepsilon$  and delay  $w$  are the QoS parameters passed to the algorithm.

#### 5.1.1. Methodology

Through analytical evaluations, we benchmark the minimum total transmit power algorithm for various different scenarios, characterized by different path compositions. We consider Rayleigh-fading links with different mean SNRs  $\bar{\gamma}_j$ . Assuming Rayleigh fading, i.e., an exponentially distributed SNR with average  $\bar{\gamma}$  at the receiver and a Shannon-based channel capacity, the Mellin transform of the service process results into [7]

$$\mathcal{M}_{g(\gamma)}(s) = e^{\frac{1}{\bar{\gamma}}} \bar{\gamma}^{s-1} \Gamma(s, \bar{\gamma}^{-1}). \quad (19)$$

where  $\Gamma(x, y) = \int_y^\infty t^{x-1} e^{-t} dt$  is the incomplete Gamma function. Substituting this in Eq. (10), the steady-state kernel for a Rayleigh-fading wireless channel is given by

$$\mathcal{K}(s, -w) = \frac{\left( e^{1/\bar{\gamma}} \bar{\gamma}^{-s} \Gamma\left(1 - s, \frac{1}{\bar{\gamma}}\right) \right)^w}{1 - \mathcal{M}_\alpha(1 + s) e^{1/\bar{\gamma}} \bar{\gamma}^{-s} \Gamma\left(1 - s, \frac{1}{\bar{\gamma}}\right)}, \quad (20)$$

for any  $s > 0$  and under the stability condition in Eq. (11). The arrival flow in this investigation is fixed to  $r_a = 20$  bits per time slot. We express link heterogeneity for a path  $\mathbb{L}$  consisting of  $N$  links using the norm of the vector  $\mathbf{l} = (l_1, \dots, l_N)$ , denoted by  $R^\mathbb{L}$  and given by:

$$R^\mathbb{L} = \sum_{j=1}^N \sum_{m=j+1}^N |l_j - l_m|, \quad (21)$$

where  $l_j$  denotes the length of link  $j$ , which reflects the path loss of the corresponding link and hence its service. Obviously, higher norm reflects higher link heterogeneity and vice versa. In the following, we consider 3-hop ( $N = 3$ ) paths with various node placements between a source and a destination located 60 m apart. Table 1 shows the exact scenarios (from almost homogeneous to strongly heterogeneous in ascending order) and their respective path norms used in the evaluations. These scenarios are deliberately chosen to highlight the effect of link heterogeneity and relative distances between intermediate nodes on network performance and the power gain obtained using the proposed power minimization algorithm compared to a naive power allocation. Since in this work we focus only on heterogeneous wireless networks, no path with norm 0 is considered. Note that in the following we refer to the link with the longest

Table 1: Considered Path Compositions

Link lengths in [m]	Path norm $R$
[20, 19, 21]	4
[20, 30, 10]	40
[5, 28, 27]	46
[20, 35, 5]	60
[5, 40, 15]	70
[5, 50.5, 4.5]	92

distance as the *critical link* (the link characterized with the highest path-loss).

In order to evaluate the efficiency of our algorithm, we are in particular interested in the total power reduction it can achieve in comparison to other approaches. For this, we consider two different comparison schemes that allocate a *uniform* power value to all links:

- *QoS-agnostic*: Each node along the path is assigned the same transmit power without considering QoS. In the numerical evaluation we use for this value the maximum available transmit power value of an IEEE 802.15.4 low-power transceiver [42], which equals  $p_{\max} = 4$  dBm.

- *QoS-aware*: In this scheme, the transmit power is iteratively reduced equally for all nodes - starting from the maximal transmit power  $p_{\max}$  - until the obtained delay violation probability is larger than the target one ( $\varepsilon$ ). Hence, as in the previous case with the QoS-agnostic scheme every node is assigned the same transmit power, however, the allocated transmit power per node is typically lower than  $p_{\max}$ .

In both chosen power allocation comparison schemes, we apply the same transmit power per node. Note that due to the different path loss per link, this results into different SNR along the path. Scenarios characterized with equal throughput among the links would implicitly require having the same average SNR along the path, which would result into homogeneously distributed channel gains. These are, however, out of the focus for this work. For all considered scenarios, we compute the minimum total transmit power as obtained from our algorithm, and compute afterwards the saving ratio or the power gain (in percent) that can be obtained in comparison to the QoS-agnostic scheme or the QoS-aware scheme. A saving of 50% indicates that through our power minimization algorithm the total transmit power is half of the value resulting from the comparison scheme.

### 5.1.2. Numerical Results

The presented results in this section are obtained via numerical computations using the algorithm presented in Section 4.1. In Fig. 4 we present the absolute required total transmit power in [mW] of our proposed algorithm for the discussed path scenarios over an increasing target delay when fixing the target delay violation probability. As the target delay is increased, the required total transmit power decreases. In addition, note that the total transmit power is higher for higher link heterogeneity. This is due to the critical link which dominates the total transmit power consumption on the path and for which the delay can only be compensated by other links up to a certain point. Note that with a maximum transmit power of 4 dBm per node, the total transmit power along the path equals 7.5357 mW. In case when even applying the maximal possible transmit power per node does not fulfill the target delay violation probability, we mark this with a straight horizontal line, as e.g. for the path with the higher heterogeneity norm.

We next present the saving gains - in Fig. 5 in comparison to the QoS-agnostic scheme and in Fig. 6 in comparison to the QoS-aware scheme. For both figures we consider the same path compositions as above and vary the target delay while keeping the target delay violation probability fixed at  $\varepsilon = 10^{-3}$ . In Fig. 5 we observe initially that all saving gains increase for an increasing target delay. This is a direct consequence from Fig. 4, as those values are compared to a fixed value of 7.5357 mW in order to determine the saving gain. Hence, it is also not surprising that the saving gain increases for more homogenous paths. In absolute terms, the saving gains are in the range of 70% to 90% which shows the potential of the proposed algorithm. If we switch over to the saving gains in comparison to the QoS-aware scheme, different observations can be made (see

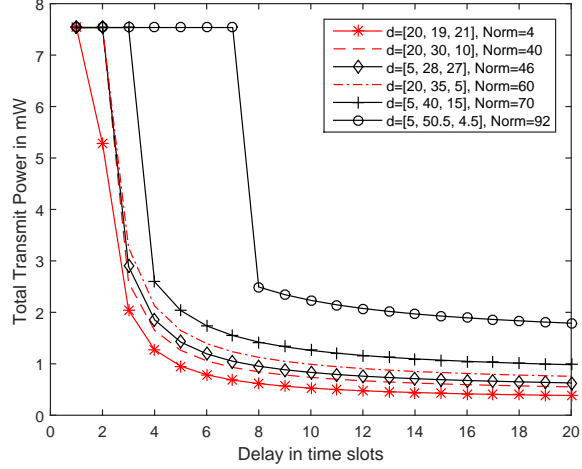


Figure 4: Sum of the total transmit power for different 3-hop paths resulting from the power-minimization algorithm over an increasing delay target. The target delay violation probability is fixed at  $\varepsilon = 10^{-3}$ .

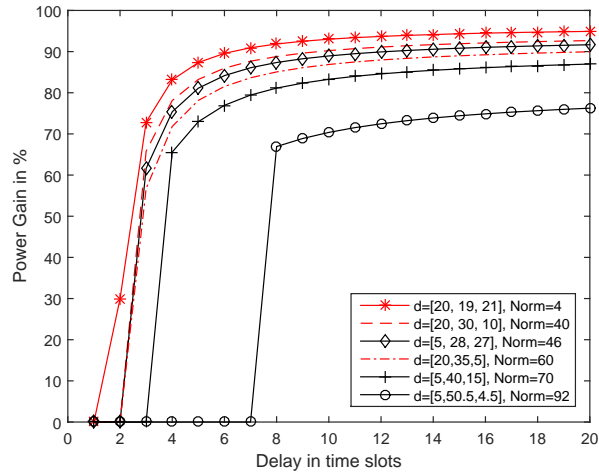


Figure 5: Saving gain of the proposed power minimization algorithm in comparison to the QoS-agnostic scheme for an increasing target delay for various 3-hop path compositions. The target delay violation probability is fixed at  $\varepsilon = 10^{-3}$ .



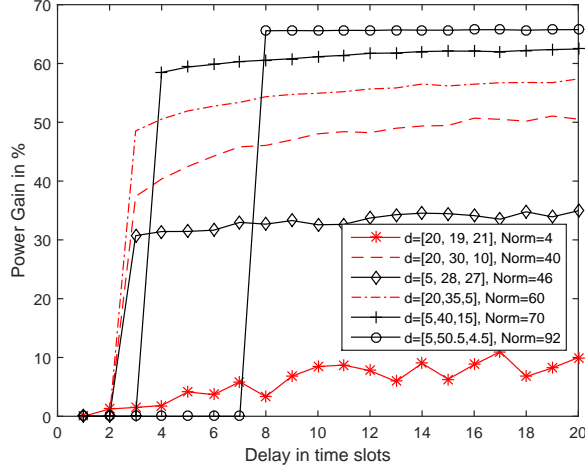


Figure 6: Saving gain of the proposed power minimization algorithm in comparison to the QoS-aware scheme for an increasing target delay for various 3-hop path compositions. The target delay violation probability is fixed at  $\varepsilon = 10^{-3}$ .

Fig. 6). Now the total power consumption varies as well for the comparison case, i.e., it drops in general for the larger target delays, while it also drops for paths with more homogenous link compositions, as otherwise the critical link in strongly heterogeneous paths dominates the power consumption and delay behavior. Therefore, in comparison to a QoS-agnostic comparison scheme, our algorithm now provides better saving gains in case of strongly heterogeneous path compositions, as only they can be significantly exploited by the proposed algorithm. In absolute terms, this leads to saving gains in the range of 10% (in case of strongly homogeneous links) up to 70% in case of strongly heterogeneous links. Again, the power gain increases as the target delay grows, but only to some particular value, since a minimal possible transmit power threshold has been reached.

Finally, in Fig. 7 we present the saving gain in comparison to the QoS-agnostic scheme in case of an increasing target delay violation probability for a fixed target delay of  $w = 10$  time slots. We notice the same trend as in Fig. 5: the smallest saving gain is around 75% for various  $\varepsilon$ . The bigger the target violation probability, the bigger is the saving gain. Also, the more heterogeneous are the paths, the smaller is the saving gain. The path with the highest norm meets the target delay for  $\varepsilon \geq 10^{-4}$  with a power gain of approx. 70%. Note that whenever the target delay or its respective violation probability could not have been fulfilled, a power gain of 0 % was obtained, represented with a horizontal line in the previous three figures (mostly for the path with  $R = 92$ ).

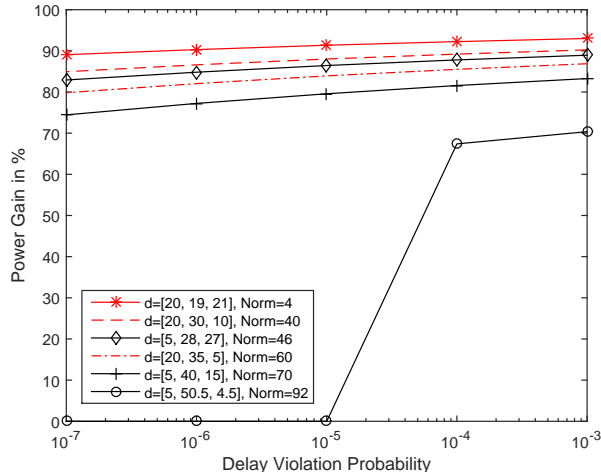


Figure 7: Saving gain of the proposed power minimization algorithm in comparison to the QoS-agnostic scheme for an increasing target delay violation probability for various 3-hop path compositions. The target delay is fixed at  $w = 10$  time slots.

### 5.1.3. Bound-Based vs. Simulation-Based Power-Minimization

Although the proposed power minimization is first of its kind, it only provides a suboptimal solution. This solution is obtained by optimizing a delay bound instead of the exact expression for the end-to-end delay violation probability, which is unfortunately unattainable. Therefore, the performance gap between the obtained bound-based power allocation scheme and the real optimum, which can only be obtained using simulation, becomes relevant for our investigation. In this section, we conduct an extensive simulation study to investigate this gap. We simulate the application in question and determine a ‘simulation-based’ optimal power allocation. We then plot the gap between the two resulting power allocations.

For this purpose, we run Algorithm 2 with parameters  $r_a = 30$  bits,  $C = 20$  symbols per time slot and for a target delay violation probability  $\varepsilon = 10^{-3}$ . The resulting power allocation is set as an initial value at each simulation. Similarly as above, we observe paths of different heterogeneity with norm  $R \in \{4, 46, 60, 70\}$ . In each iteration the delay violation probability was obtained by a simulation. The simulation follows the same approach as defined in the algorithm: by computing the minimal gradient of the simulated delay violation probability (as in line 12 in Algorithm 2), the link whose transmit power has to be reduced in each iteration by a certain  $\Delta p$  is determined. Whenever no further reduction of the transmit power on any of the links is possible, i.e., the resulting delay violation probability is bigger than the target one,  $\Delta p$  is halved. This is done maximum 15 times, i.e.,  $\Delta p$  is reduced by a factor of  $2^{15}$ . The initial value of

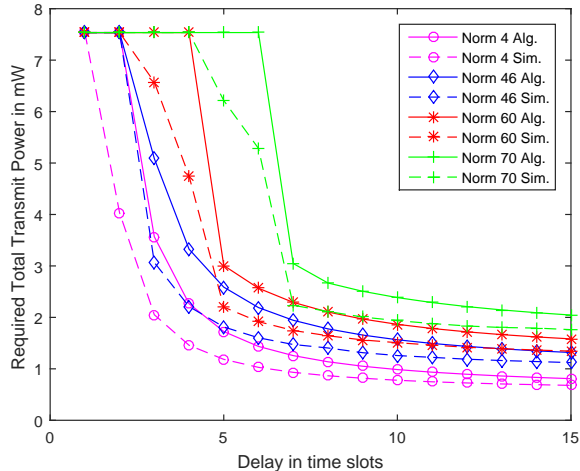


Figure 8: Required total transmit power along all nodes of various 3-hop paths. The dotted lines represent the total transmit power in case when the optimal point of power and delay under given target delay constraints is obtained via simulations. The target delay violation probability is fixed at  $\varepsilon = 10^{-3}$ .

$$\Delta p = 0.01 \text{ mW}^5.$$

In this way, we continue reducing the transmit power on the links along the path, beyond the one suggested by the algorithm. This approach enables us to characterize the gap between the total transmit power computed by the proposed bound-based power minimization in comparison to the total transmit power obtained via simulations of the analogous process, s.t. the resulting simulated delay violation probability is close to  $\varepsilon$  from below. We illustrate this additional power saving in Fig. 8 and Fig. 9. The former figure depicts the difference between the total transmit power obtained by the algorithm and the one obtained with simulations in absolute terms. A total transmit power of 7.5357 mW represents the cases for which applying even the maximal possible transmit power of 4 dBm (approx. 2.5 mW) per node does not result into meeting the desired target delay. We notice that, in absolute terms, the additional decrease of the total transmit power while performing system-based optimization is rather small for all scenarios, which highlights the efficiency of our proposed algorithm. We further notice that in some link heterogeneity scenarios the simulation fulfills the target delay sooner than the forecast analytical approach (see e.g. the path with  $R = 70$ : For  $w = 5$  the simulation achieves the target delay violation probability of  $10^{-3}$  with total transmit power smaller than

<sup>5</sup>We stress again that, by applying small  $\Delta p$  steps we make sure that the obtained power vector (and its resulting kernel) lies very close to the actual optimal transmit power solution for the considered scenario.

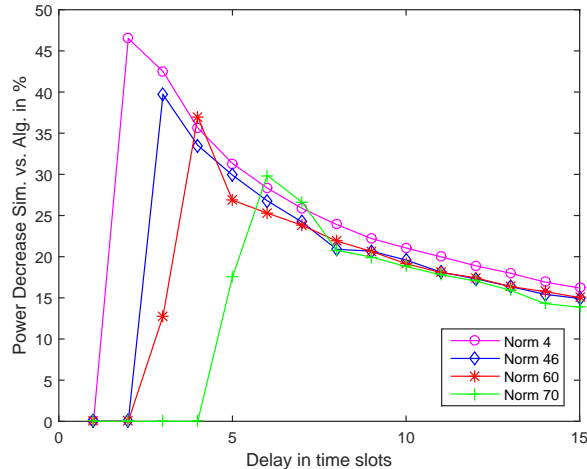


Figure 9: Additional decrease of the total transmit power suggested by the bound-based algorithm when performing simulations. The target delay violation probability is  $\varepsilon = 10^{-3}$ .

7.5357 mW, while the analysis fails to achieve the demanded QoS for the same target delay even with the maximal transmit power). This behaviour results from the gap between the analysis and the simulation.

Fig. 9 represents the additional power gain w.r.t. the total transmit power obtained from the described approach. An additional power decrease of 0 % means that obtaining the optimal transmit power by simulations does not lead to any additional power savings in comparison to the proposed algorithms. In cases of strict QoS requirements applying even a maximum power of 4 dBm per link will not satisfy the target statistical delay constraints for both the simulation and the analytical approach. In all other cases the simulation meets the target delay violation probability. As it can be seen, while the power gain is as big as 47% for paths of low heterogeneity and small target delays, it converges to around 15% for longer delays for diverse path heterogeneity. This means, that for looser delay constraints, the actual system optimum, if obtained by simulations, will enable an additional 15% decrease in the total transmit power in comparison to the bound-based power minimization. This power gap is generally significantly smaller for more heterogeneous paths.

Note however, that, even if a further decrease of the total power by more than 15% is observed for various scenarios, the proposed bound-based power-minimization algorithm can be used as a good estimate on the system performance, providing at a same time delay guarantees. Moreover, applying the suggested transmit power allocation by the algorithm leads to an improved performance, due to the lower resulting delay violation probability. Such bound-based optimization is especially important for applications with strict QoS demands,

introducing a so called *safety gap* in the actual system performance.

### 5.2. Evaluation of the Lifetime Maximization Algorithm

We evaluate in this subsection the second proposed algorithm from Sec. 4.2, which takes the battery state of the nodes into account and maximizes the lifetime of the network by modifying the transmit power settings per node. As this scenario and objective is more relevant in practice, we also consider a more practical channel capacity function in this section and resort to the WirelessHART industrial standard [43], widely used for process automation applications with battery-powered devices. In order to apply our proposed algorithm, we use the provided corresponding kernel given in [44], defined according to the physical layer description and BER stated in the IEEE 802.15.4-2006 standard [41]<sup>6</sup>. In the following subsections we first explain our methodology and then discuss some numerical results presenting insights on how QoS-aware power management can improve network lifetime under both link and battery state heterogeneity.

#### 5.2.1. Methodology

Let  $N_s$  be the number of time slots within a superframe, while a time slot lasts for  $T = 10$  ms according to WirelessHART. We hence present the delay in number of superframes, where a superframe lasts for  $T \cdot N_s$  ms. We assume a round-robin link scheduling fashion, where the  $j$ -th time slot within one superframe is assigned to the  $j$ -th link along the path, while the channel gain varies randomly in each time slot, i.e., we assume block fading. The subsequent channel gains along the path are, however, independent on each other, due to the frequency-hopping applied on the MAC layer in WirelessHART.

The kernel of a single-hop WirelessHART system is given by [44]:

$$\mathcal{K}(s, -w) = \frac{(1 + (e^{-k_a s} - 1)Q(\bar{\gamma}))^w}{1 - e^{r_a s} (1 + (e^{-k_a s} - 1)Q(\bar{\gamma}))}, \quad (22)$$

under the stability condition

$$\begin{aligned} e^{r_a s} (1 + (e^{-k_a s} - 1)Q(\bar{\gamma})) &< 1 \\ \Leftrightarrow r_a &< -\frac{1}{s} \log(1 + (e^{-k_a s} - 1)Q(\bar{\gamma})), \end{aligned} \quad (23)$$

where  $k_a$  represents the maximal number of bits that can be transmitted in a WirelessHART time slot (or the MAC frame size),  $r_a$  is the size of the payload generated at the beginning of each superframe by the application and  $Q(\bar{\gamma})$  is the probability of successful MAC frame transmission over the wireless link, given as a function of the BER and the average SNR [41]. The result in Eq. (22) is explicitly derived in [44] and serves as basis for the following numerical evaluation. The end-to-end kernel is obtained when the single-hop kernel is substituted into Eq. (16).

---

<sup>6</sup>Note that this is no longer the active standard, since the 802.15.4-2015 is the newest version. However, the WirelessHART radios comply with IEEE 802.15.4-2006.

### 5.2.2. Numerical Results

In the following, we are mainly interested in the network lifetime extension, represented in %, obtained when applying our bound-based lifetime maximization algorithm (Algorithm 3 in Appendix A) in comparison to the QoS-agnostic scheme. The lifetime is obtained as the minimal time duration a node can be operated by its corresponding battery among all node lifetimes for a given multi-hop path. The investigation is done for different target delays (in terms of superframes). We set  $k_a = 127$  byte and the payload size  $r_a$  is 10 byte<sup>7</sup>. The arrival rate at the source node is one payload per superframe.

To parametrize the transceiver model, we turn to the low-power Atmel IEEE802.15.4-based transceiver AT86RF233 [42]. This transceiver is either in idle, send or receive mode and we obtain the power consumption in these modes from the given data sheet<sup>8</sup>. Other system parameters are summarized in Table 2.

Table 2: System Parameters

Name	Value
Total distance	60 m
Payload size	10 bytes
Frame size	127 bytes
Delay violation probability $\varepsilon$	$10^{-3}$
Maximal transmit power $p_{\max}$	4 dBm
Current consumption in idle mode	$0.2 \mu\text{A}$
Current consumption in Rx mode	11.8 mA
Time slot duration	10 ms
Time spent in Tx mode	4.256 ms
ACK duration	0.8 ms

For the evaluations, we again consider different multi-hop path compositions as in Table 1. However, as the battery state is another important parameter regarding the performance of the lifetime extension algorithm, we consider in addition three settings of the battery states. In the *equal* case, the battery of each node is fully charged at the moment of algorithm execution. The *proportional* case assumes a proportional battery full state distribution among the nodes regarding the path loss on the link, i.e., the link with the highest path-loss is assigned the most charged battery. We finally consider the *inverse proportional* battery state allocation, where the link with the highest path loss is allocated the least charged battery. All presented results refer to a target delay viola-

<sup>7</sup>Small packets are typical for process automation applications.

<sup>8</sup>Note that transceivers can offer only discrete transmit power values. Moreover, the provided data sheet contains current consumption data only for three power thresholds. For this reason, we perform polynomial curve fitting in order to obtain higher resolution consumption data and get more abstract results, not necessarily matching the transceiver capabilities in total. However, we do stay in the offered transmit power span.

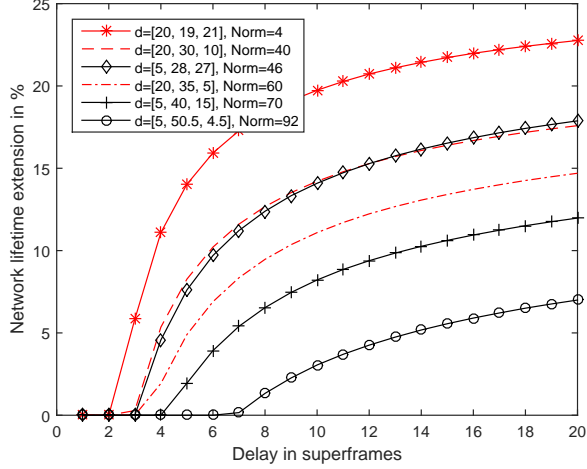


Figure 10: Network lifetime extension for different target delays and path compositions. An equal battery state charge is assumed among all links.

tion probability of  $10^{-3}$  and are compared to the QoS-agnostic power allocation scheme.

Fig. 10 shows the gain of the network lifetime extension algorithm for different delay target  $w$  considering the above discussed 3-hop path scenarios with various path norm  $R$ . Note that for 3-hop paths, the superframe duration is 30 ms. In this plot, we consider the equal battery state charge among all nodes. For lower delays there is small gain in the network lifetime when using the algorithm in comparison to the QoS-agnostic scheme. As the target delay is increased, the gain in network lifetime increases. As we notice in Fig. 10, the more heterogeneous the links are, the less one can benefit from the proposed bound-based algorithm. The path with the least lifetime gain is the path with the biggest path norm.

Fig. 11 illustrates the gain in network lifetime in case of proportional initial battery state distribution. We now notice a different trend: The paths with higher link heterogeneity benefit more from the lifetime maximization algorithm than paths with lower norm. This is due to the fact that the links with lower path loss (the better links) have a lower battery state and therefore are given advantage in the power-minimization decision, resulting finally with lower assigned transmit power and longer network lifetime. Note however, that the lowest lifetime extension is obtained for the path [5, 28, 27], with the third link being the critical one (consuming the most energy, since it both sends and receives packets) and not the first one.

Fig. 12 shows the network lifetime extension considering the same path scenarios for an inverse proportional initial battery state allocation, where the node in front of the weakest link is allocated the least battery capacity. We now no-

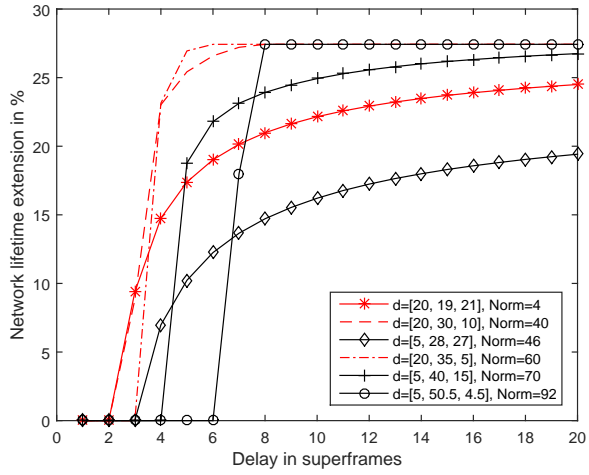


Figure 11: Network lifetime extension for different target delays and path compositions. A proportional battery state charge is assumed among all links.

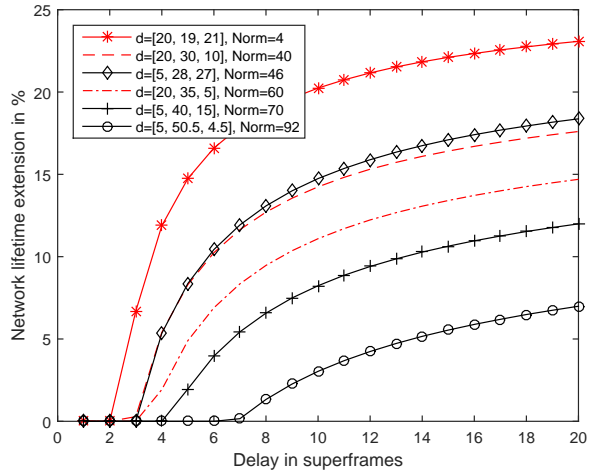


Figure 12: Network lifetime extension for different target delays and path compositions. An inverse proportional battery state charge is assumed among all links.



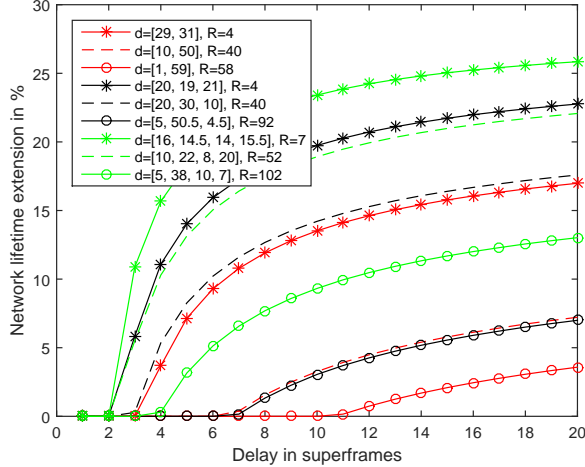


Figure 13: Network lifetime extension for different target delays and path compositions for 2-, 3-, and 4-hop paths. An equal battery state charge is assumed among all links.

tice the same trend as in the case of equal battery state allocation, namely that more homogeneous paths result with a larger lifetime extension. This is expected, since in both cases the algorithm prefers the links which consume more energy (i.e., the higher path loss links) when making the decision which link's transmit power to decrease.

Finally, in Fig. 13 we show the network lifetime extension for 2-, 3- and 4-hop paths, each of them having low, moderate and high path norms. The initial battery allocation is equal among all nodes. We notice that the lifetime extension increases with the number of hops, however, still yielding the best one for paths with almost equal link path loss, similar to the observations in Fig. 10 and Fig. 12. Hence, as the path length grows, an optimal transmit power allocation under delay constraints becomes more necessary, even for rather low link heterogeneity.

The motivation behind the proposed investigation is the following: Knowing how the power minimization influences the network lifetime extension depending on the battery full-state allocation, will enable better network design i.e., node placement decision. The algorithm is usually executed at the beginning of network operation, when all batteries have equal full-state. For example, knowing that paths consisting of homogeneous links (links with similar average SNR) benefit more from a power management scheme, a network designer will make sure that the wireless industrial network he is planning contains primarily homogeneous paths. After the network nodes have been running for a while, their batteries get depleted, which changes the battery full-state allocation along a given path from equal to inversely proportional one (the links with the high-

est path loss incorporate the least charged battery). This transition from one allocation to the other is expected if the data load is equal between all nodes in the network. Here again, paths with smaller degree of heterogeneity benefit more from the power minimization scheme. Therefore, more homogeneous paths should be preferred in routing decisions which are being constantly made during network operation.

Finally, as a result to a routing algorithm, it might happen that a route between two nodes is changed, s.t. we now observe proportional battery allocation along the respective path. In this case, performing power minimization while considering the proportional battery full-state allocation will extend the network lifetime especially in case of highly heterogeneous paths. Hence, such paths should be preferred by the routing algorithm, since they will significantly maximize the network lifetime in comparison to the rather homogeneous paths. Thus, combining these insights obtained by the battery allocation evaluation within a routing algorithm or a network design phase, will lead to power-efficient network performance while at the same time providing end-to-end delay guarantees in a wireless multi-hop industrial network.

### 5.2.3. Bound-Based vs. Simulation-Based Lifetime Maximization

Similarly as in Section 5.1.3, we now provide a quantitative illustration of the gap between the bound-based and the simulation-based lifetime maximization. The simulation is started with a power allocation resulting from Algorithm 3, using the same system parameters as given in Table 2. In each iteration, the node whose transmit power is going to be reduced is chosen as the node with the least remaining battery lifetime. We are interested by how much the network lifetime can be additionally increased if using a simulation-based approach in comparison to the network lifetime provided by the bound-based method. In the presented results, we make sure that the simulation fulfills the target delay violation probability, except for the cases when even applying the maximal possible transmit power of 4 dBm does not suffice. This is marked by a horizontal line in the figures. We first take a look at the absolute values of the minimal battery duration of both schemes for lifetime maximization, shown in Fig. 14. The same link heterogeneity of 3-hop paths, as in Section 5.1.3, is considered. We notice that the minimal battery duration provided by the bound-based algorithm lies very closely to the one provided by simulations.

Fig. 15 shows the additional gain in network lifetime if simulation-based instead of bound-based power optimization is applied. In comparison to the total transmit power minimization, in the WirelessHART case study we observe much smaller additional gain in the network lifetime (not bigger than 7 %) when conducting simulations. This verifies the usefulness of the proposed algorithm for lifetime maximization, which at the same time provides performance guarantees of wireless networks employed in practice. Since the power consumed in transmit mode is only one of the factors influencing the whole battery energy consumption, the optimal power allocation for a WirelessHART multi-hop network can be very closely estimated by a solution based on the end-to-end delay

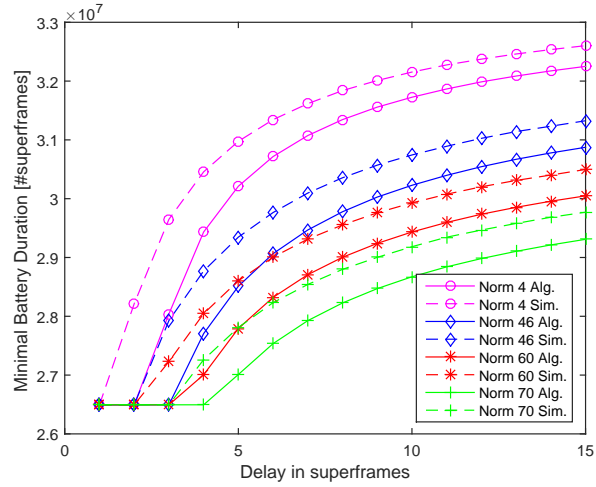


Figure 14: A minimal battery duration in number of superframes vs. target delay  $w$  resulting from both the bound-based and the simulation-based lifetime maximization.

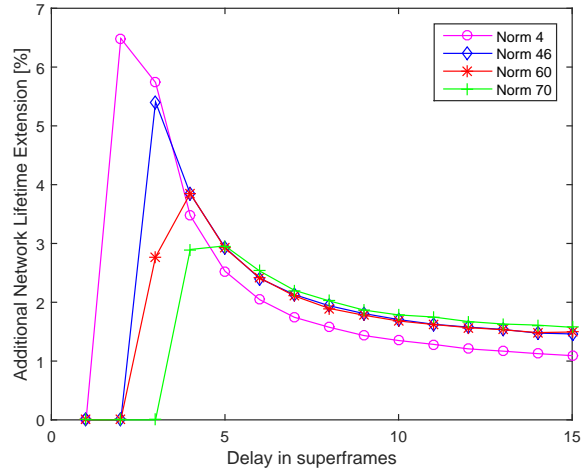


Figure 15: Additional gain in the network lifetime extension for different target delays when using simulations in comparison to the delay bound-based approach.

bound. This holds especially for paths with higher degree of link heterogeneity, as shown in the figure.

## 6. Conclusion

This paper presents a novel bound-based algorithm for transmit power allocation with two variants: (i) total power minimization, and, (ii) network lifetime maximization, in wireless industrial networks. These algorithms are based on theoretical results that we developed for the performance of heterogeneous (where both channel gain and battery full state heterogeneity are considered) multi-hop wireless networks using a stochastic network calculus approach. We provide numerical evaluation of the performance of these algorithms and compare them to simulation-based power optimization.

We consider two wireless channel capacity models: (1) an ‘ideal’ Shannon-capacity-based model, and, (2) a ‘realistic’ WirelessHART-based model, the latter of which is widely applied in real industrial systems used for process automation. The numerical analysis of our proposed bound-based power optimization shows a power gain of up to 95% for almost homogeneous multi-hop paths and more than 70% even for paths with highly heterogeneous links using the ideal capacity model (1) above. It also shows that the power gain is high even for stricter delay violation probability requirements. A second group of numerical results, pertaining to the capacity model in (2) above, shows network lifetime extension of up to 25% for various link heterogeneity and types of initial battery allocation strategies. We conclude that for nodes having equal battery capacities, the paths with higher link homogeneity benefit more of the proposed battery-lifetime maximization approach. However, in case of a different battery allocation strategy, higher lifetime extension is obtained for multi-hop paths with higher degree of link heterogeneity.

Finally, to evaluate the accuracy of the proposed bound-based optimization, we provide a quantitative evaluation of the gap between the optimal power allocation resulting from the bound-based approach and the one obtained via simulation of the application in question. Although the gap between the bound-based and the simulation-based optimum is non-negligible for smaller target delays in case of total transmit power minimization, there is an insignificant difference between the two approaches in case of network lifetime maximization. Hence, we strongly believe that the presented algorithms for bound-based optimal transmit power allocation based on stochastic network calculus principles, being first of their kind, offer a useful analytical framework for the design of wireless multi-hop networks under statistical delay constraints. Furthermore, the recursive nature of the devised end-to-end delay bound together with the power minimization algorithms presents a solid basis for the development of energy-efficient, delay-aware routing algorithms for future wireless multi-hop heterogeneous networks.

An important extension of this work relates perhaps to the analysis of networks being exposed to multiple flows, as in meshed networks. Our presented approach is applicable even for such networks as long as flows utilize orthogonal

resources which can be reserved per node, as is realized in WirelessHART or through approaches like Time-Sensitive Networking. Otherwise, if the routing path is not determined, and also no resources are reserved for the flow under consideration, we provide a worst-case bound on a single flow being exposed to cross-traffic. This result nevertheless has to be extended towards multi-path routing, which constitutes a next step in the evolution of the framework presented here.

## APPENDIX

### Appendix A. Pseudo Codes of the Bound-Based Algorithms

In this appendix we present the pseudo-code for the bound-based power-minimization algorithm (Algorithm 2) and the bound-based network lifetime extension algorithm (Algorithm 3). The function *search\_s* (Algorithm 1) is an auxiliary function called in both algorithms.

---

**Algorithm 1** Search  $s^* \in (0, b)$  for which  $\mathcal{K}^{\mathbb{L}}(s^*, -w)$  is minimal

---

```

1: function SEARCH_S ( $0, b, \bar{\gamma}, \Delta_{\min}, r_a, w$ )
Ensure: Find  $s^*$ 
2:   Compute  $s_1, s_m, s_r \in (0, b)$ 
3:    $s_{\text{start}} = 0, s_{\text{end}} = b$ ; use for simplicity  $\mathcal{K}^{\mathbb{L}}(s, -w) \triangleq \mathcal{K}^{\mathbb{L}}(s)$ 
4:   if  $s_m - s_1 > \Delta_{\min}$  then
5:     Find out in which interval lies  $s^*$ 
6:     ***Case 1:  $s^* \in (s_{\text{start}}, s_m)$ 
7:     if  $\mathcal{K}^{\mathbb{L}}(s_{\text{end}}) > \mathcal{K}^{\mathbb{L}}(s_r) > \mathcal{K}^{\mathbb{L}}(s_m) > \mathcal{K}^{\mathbb{L}}(s_1)$  then
8:        $s^* = \text{search\_s}(s_{\text{start}}, s_m, \bar{\gamma}, \Delta_{\min}, k_{\text{ts}}, w)$ 
9:     ***Case 2:  $s^* \in (s_m, s_{\text{end}})$ 
10:    else if  $\mathcal{K}^{\mathbb{L}}(s_{\text{start}}) > \mathcal{K}^{\mathbb{L}}(s_1) > \mathcal{K}^{\mathbb{L}}(s_m) > \mathcal{K}^{\mathbb{L}}(s_r)$  then
11:       $s^* = \text{search\_s}(s_m, s_{\text{end}}, \bar{\gamma}, \Delta_{\min}, k_{\text{ts}}, w)$ 
12:    ***Case 3:  $s^* \in (s_1, s_r)$ 
13:    else if  $\mathcal{K}^{\mathbb{L}}(s_{\text{end}}) > \mathcal{K}^{\mathbb{L}}(s_r) > \mathcal{K}^{\mathbb{L}}(s_m)$ 
14:      AND  $\mathcal{K}^{\mathbb{L}}(s_{\text{start}}) > \mathcal{K}^{\mathbb{L}}(s_1) > \mathcal{K}^{\mathbb{L}}(s_m)$  then
15:         $s^* = \text{search\_s}(s_1, s_r, \bar{\gamma}, \Delta_{\min}, k_{\text{ts}}, w)$ 
16:      end if
17:    else
18:       $s^* = s_m$ 
19:    return
20:  end if
21: end function

```

---

---

**Algorithm 2** Transmit Power-Minimization Algorithm
 

---

**Require:**  $|\vec{h}^2|, \Delta p, p_{\max}, \Delta p_{\min}, r_a, w, \varepsilon, \Delta \varepsilon$

**Ensure:**  $\min \sum_{j=1}^N p_j$ , s.t.  $\mathcal{K}^{\mathbb{L}}(s, -w) \leq \varepsilon$

- 1:  $\vec{p} = p_{\max}; \bar{\gamma} = \min\{\bar{\gamma}_{\max}\} = \min[f(p_{\max}, |\vec{h}^2|); \mathcal{K}^{\mathbb{L}}(s, -w) \triangleq \mathcal{K}^{\mathbb{L}}(s, \vec{p})$
  - 2: Find  $s', \forall s \in (0, s')$ , s.t. Eq. (11) holds for  $\bar{\gamma}$
  - 3: Compute  $\vec{P}_{\text{txmin}}$ , s.t. channel capacity  $\geq r_a$
  - 4: Compute current delay bound  $\hat{\varepsilon} = \mathcal{K}^{\mathbb{L}}(s, \vec{p})$
  - 5: **if** ( $\hat{\varepsilon} > \varepsilon$ ) **then return fail**
  - 6: **else**
  - 7:     **while** ( $\hat{\varepsilon} \notin (\varepsilon - \Delta \varepsilon, \varepsilon)$ ) **do**
  - 8:         **while** ( $\hat{\varepsilon} > \varepsilon$ ) AND ( $\Delta p > \Delta p_{\min}$ ) **do**
  - 9:             Choose smaller  $\Delta p : \Delta p = \Delta p/2$
  - 10:         **end while**
  - 11:          $\vec{p}' = \vec{p}; \vec{p}'_j$  is transmit power vector where  $p_j = p'_j - \Delta p$
  - 12:         Find the smallest gradient:  $j = \underset{N}{\operatorname{argmin}} \nabla \mathcal{K}_j = \left| \frac{\hat{\varepsilon} - \mathcal{K}^{\mathbb{L}}(s, \vec{p}'_j)}{\Delta p} \right|$
  - 13:          $p'_j = p_j - \Delta p$ , assure  $p'_j \geq p_{\min j}; \bar{\gamma} = f(\vec{p}', |\vec{h}^2|)$
  - 14:          $s^* = \text{search}_s(s_{\text{start}}, b, \bar{\gamma}, \Delta_{\min}, r_a, w)$ ; compute  $\hat{\varepsilon} = \mathcal{K}^{\mathbb{L}}(s^*, \vec{p}')$
  - 15:          $\vec{p} = \vec{p}'$
  - 16:         **end while**
  - 17:         **return**  $\vec{p}$
  - 18: **end if**
- 

---

**Algorithm 3** Network Lifetime Maximization Algorithm
 

---

**Require:**  $|\vec{h}^2|, \Delta p, p_{\max}, \Delta p_{\min}, k_a, r_a, w, \varepsilon, \Delta \varepsilon, \vec{B}$

**Ensure:**  $\max \min_j \{\theta_j\}, \theta_j \in \vec{\theta}, \vec{\theta} = \frac{\vec{B}}{T\vec{p}}, \mathcal{K}^{\mathbb{L}}(s, -w) \leq \varepsilon$

- 1:  $\vec{p} = p_{\max}; \bar{\gamma} = \min\{\bar{\gamma}_{\max}\}$
  - 2: Find  $s', \forall s \in (0, s')$  stability condition Eq. (11) holds for  $\bar{\gamma}$
  - 3: Set  $P_{\text{txmin}}$  to transceiver capabilities;  $\hat{\varepsilon} = \mathcal{K}^{\mathbb{L}}(s, -w)$
  - 4: Same approach as in Algorithm 2, only replace line 11 and 12 with
  - 5:  $M = \forall j : \{\underset{j}{\operatorname{argmin}}\{\theta_j\}\}, \forall j \in M : p'_j = p_j - \frac{\Delta p}{|M|}$ , assure  $p'_j \geq p_{\min}$
-

## Appendix B. Proof of the Delay Bound Convexity

**Proof 2.** As shown in Eq. (10), the kernel has the following form:

$$\begin{aligned} \mathcal{K}(s, -w) &= \frac{\mathcal{M}_{g(\gamma)}^w(1-s)}{1 - \mathcal{M}_\alpha(1+s)\mathcal{M}_{g(\gamma)}(1-s)} \\ &= \frac{(\mathcal{M}_S(1-s, \tau, t))^w}{1 - \mathcal{M}_A(1+s, \tau, t)\mathcal{M}_S(1-s, \tau, t)}, \end{aligned} \quad (\text{B.1})$$

where  $\mathcal{M}_A(1+s, \tau, t)$  is the Mellin transform of the arrival process in  $1+s$  and  $\mathcal{M}_S(1-s, \tau, t)$  is the Mellin transform of the service in  $1-s$ . From its definition it follows that,  $\mathcal{M}_A(1+s, \tau, t)$  is strictly increasing and  $\mathcal{M}_S(1-s, \tau, t)$  is strictly decreasing in  $s$ . Note that we limit in the following the scope of the parameter  $s$  to the stability region, i.e.,  $s \in (0, b)$ . In order to prove that Eq. (B.1) is convex, we will first show that  $\mathcal{M}_A(1+s, \tau, t) \cdot \mathcal{M}_S(1-s, \tau, t)$  is convex. We will then use this fact to prove the convexity of the whole kernel.

Let us consider the following functions:

$$\begin{aligned} \mathcal{M}_A(1+s, \tau, t) &= (\mathbb{E}[e^{s\alpha}])^{t-\tau} \\ \mathcal{M}_S(1-s, \tau, t) &= (\mathbb{E}[e^{-s\beta}])^{t-\tau}, \end{aligned} \quad (\text{B.2})$$

where  $\alpha$  and  $\beta$  are the random arrival to the link and service offered by the link, respectively. Note here that,  $(\mathbb{E}[e^{-s\beta}])^{t-\tau} \leq 1$  for  $s \in (0, b)$ , i.e., the Mellin transform of the service reaches its maximum for  $s = 0$ . In the following we will prove that  $(\mathbb{E}[e^{s\alpha}])^{t-\tau} \cdot (\mathbb{E}[e^{-s\beta}])^{t-\tau}$  is convex in  $s$  for the range of  $s$  for which the stability condition holds.

We start by rewriting the product as

$$(\mathbb{E}[e^{s\alpha}])^{t-\tau} \cdot (\mathbb{E}[e^{-s\beta}])^{t-\tau} = (\mathbb{E}[e^{-sx}])^{t-\tau} < 1, \quad (\text{B.3})$$

where we substitute  $x = \beta - \alpha$  and use the independence of  $\alpha$  and  $\beta$ . In order for  $(\mathbb{E}[e^{-sx}])^{t-\tau}$  to be convex, it has to hold for any  $0 \leq \delta \leq 1$ :

$$\left(\mathbb{E}[e^{-(\delta s_1 + (1-\delta)s_2)x}]\right)^{t-\tau} \leq \delta (\mathbb{E}[e^{-s_1 x}])^{t-\tau} + (1-\delta) (\mathbb{E}[e^{-s_2 x}])^{t-\tau}. \quad (\text{B.4})$$

Let us apply Hölder's inequality [45] to the left-hand side of Eq. (B.4). Hölder's inequality states that

$$\mathbb{E}[|X \cdot Y|] \leq (\mathbb{E}|X|^p)^{1/p} \cdot (\mathbb{E}|Y|^q)^{1/q} \quad (\text{B.5})$$

for  $\forall p, q$  for which  $\frac{1}{p} + \frac{1}{q} = 1$ . Hence, for  $\frac{1}{p} = \delta$  and  $\frac{1}{q} = 1 - \delta$ , we have:

$$\begin{aligned} \left(\mathbb{E}[e^{-(\delta s_1 + (1-\delta)s_2)x}]\right)^{t-\tau} &= \left(\mathbb{E}[|e^{-\delta s_1 x} \cdot e^{-(1-\delta)s_2 x}|\right])^{t-\tau} \\ &\leq \left(\mathbb{E}[|e^{-\delta s_1 x}|^{1/\delta}]\right)^{(t-\tau)\delta} \cdot \left(\mathbb{E}[|e^{-(1-\delta)s_2 x}|^{1/(1-\delta)}]\right)^{(t-\tau)(1-\delta)} \\ &= (\mathbb{E}[e^{-s_1 x}])^{(t-\tau)\delta} \cdot (\mathbb{E}[e^{-s_2 x}])^{(t-\tau)(1-\delta)} \\ &\leq \delta (\mathbb{E}[e^{-s_1 x}])^{t-\tau} + (1-\delta) (\mathbb{E}[e^{-s_2 x}])^{t-\tau}. \end{aligned} \quad (\text{B.6})$$

In the last line we use the fact that

$$u^\delta v^{1-\delta} \leq \delta u + (1-\delta)v, \forall \delta \in [0, 1], \quad (\text{B.7})$$

which holds because of the following: Let us define  $f(\delta) = u^\delta v^{1-\delta} - \delta u - (1-\delta)v$ . The second derivative of  $f(\delta)$  results to:

$$f''(\delta) = u^\delta v^{1-\delta} (\log(u) - \log(v))^2 \geq 0, \quad (\text{B.8})$$

$\forall \delta \in [0, 1]$  and  $u, v < 1$ . Since  $f(0) = f(1) = 0$  and  $f''(\delta) \geq 0$ , it follows that  $f(\delta)$  reaches a local minimum for  $\delta \in [0, 1]$ . Hence,  $f(\delta) \leq 0, \forall \delta \in [0, 1]$  and therefore Eq. (B.7) holds. Therefore, we show that  $\mathcal{M}_{\mathcal{A}}(1+s, \tau, t) \mathcal{M}_{\mathcal{S}}(1-s, \tau, t)$  is convex. Having shown this, it follows that the function

$1 - \mathcal{M}_{\mathcal{A}}(1+s, \tau, t) \mathcal{M}_{\mathcal{S}}(1-s, \tau, t)$  is concave and positive, since  $\mathcal{M}_{\mathcal{A}}(1+s, \tau, t) \mathcal{M}_{\mathcal{S}}(1-s, \tau, t) \leq 1$  due to the stability condition. Hence, the reciprocal is convex, i.e.,  $\frac{1}{1 - \mathcal{M}_{\mathcal{A}}(1+s, \tau, t) \mathcal{M}_{\mathcal{S}}(1-s, \tau, t)}$  is convex [46].

We now turn to the second part of the proof, namely, we consider the entire kernel. In order to show that the kernel given with Eq. (B.1) is convex, it has to hold:

$$\begin{aligned} & \frac{(\mathbb{E}[e^{-(\delta s_1 + (1-\delta)s_2)\beta}])^{(t-\tau)w}}{1 - (\mathbb{E}[e^{(\delta s_1 + (1-\delta)s_2)\alpha}] \cdot \mathbb{E}[e^{-(\delta s_1 + (1-\delta)s_2)\beta}])^{t-\tau}} \\ & \leq \delta \cdot \frac{(\mathbb{E}[e^{-s_1\beta}]^{(t-\tau)w}}{1 - (\mathbb{E}[e^{s_1\alpha}] \cdot \mathbb{E}[e^{-s_1\beta}])^{t-\tau}} + (1-\delta) \cdot \frac{(\mathbb{E}[e^{-s_2\beta}]^{(t-\tau)w}}{1 - (\mathbb{E}[e^{s_2\alpha}] \cdot \mathbb{E}[e^{-s_2\beta}])^{t-\tau}}, \end{aligned} \quad (\text{B.9})$$

$\forall s_1, s_2 \in (0, b)$  and  $0 \leq \delta \leq 1$ . Since  $\frac{1}{1 - \mathcal{M}_{\mathcal{A}}(1+s, \tau, t) \cdot \mathcal{M}_{\mathcal{S}}(1-s, \tau, t)}$  is convex, we know:

$$\begin{aligned} & \frac{1}{1 - (\mathbb{E}[e^{(\delta s_1 + (1-\delta)s_2)\alpha}] \cdot \mathbb{E}[e^{-(\delta s_1 + (1-\delta)s_2)\beta}])^{t-\tau}} \\ & \leq \delta \cdot \frac{1}{1 - (\mathbb{E}[e^{s_1\alpha}] \cdot \mathbb{E}[e^{-s_1\beta}])^{t-\tau}} + (1-\delta) \cdot \frac{1}{1 - (\mathbb{E}[e^{s_2\alpha}] \cdot \mathbb{E}[e^{-s_2\beta}])^{t-\tau}}. \end{aligned} \quad (\text{B.10})$$

Multiplying the left- and right-hand side of Eq. (B.10) by  $(\mathbb{E}[e^{-(\delta s_1 + (1-\delta)s_2)\beta}])^{(t-\tau)w}$ , we obtain:

$$\begin{aligned} & \frac{(\mathbb{E}[e^{-(\delta s_1 + (1-\delta)s_2)\beta}])^{(t-\tau)w}}{1 - (\mathbb{E}[e^{(\delta s_1 + (1-\delta)s_2)\alpha}] \cdot \mathbb{E}[e^{-(\delta s_1 + (1-\delta)s_2)\beta}])^{t-\tau}} \\ & \leq \delta \cdot \frac{(\mathbb{E}[e^{-(\delta s_1 + (1-\delta)s_2)\beta}])^{(t-\tau)w}}{1 - (\mathbb{E}[e^{s_1\alpha}] \cdot \mathbb{E}[e^{-s_1\beta}])^{t-\tau}} + (1-\delta) \cdot \frac{(\mathbb{E}[e^{-(\delta s_1 + (1-\delta)s_2)\beta}])^{(t-\tau)w}}{1 - (\mathbb{E}[e^{s_2\alpha}] \cdot \mathbb{E}[e^{-s_2\beta}])^{t-\tau}}. \end{aligned} \quad (\text{B.11})$$



Now, using again Hölder's inequality for  $\frac{1}{p} = \delta$  and  $\frac{1}{q} = 1 - \delta$ , we obtain:

$$\begin{aligned}
& \left( \mathbb{E}[e^{-(\delta s_1 + (1-\delta)s_2)\beta}] \right)^{(t-\tau)w} = \left( \mathbb{E}[|e^{-\delta s_1 \beta}| \cdot |e^{-(1-\delta)s_2 \beta}|] \right)^{(t-\tau)w} \\
& \leq \left( \mathbb{E}[|e^{-\delta s_1 \beta}|^{1/\delta}] \right)^{(t-\tau)w\delta} \cdot \left( \mathbb{E}[|e^{-(1-\delta)s_2 \beta}|^{1/(1-\delta)}] \right)^{(t-\tau)w(1-\delta)} \\
& = \left( \mathbb{E}[|e^{-s_1 \beta}|] \right)^{(t-\tau)w\delta} \cdot \left( \mathbb{E}[|e^{-s_2 \beta}|] \right)^{(t-\tau)w(1-\delta)} \\
& \leq \left( \mathbb{E}[|e^{-s_1 \beta}|] \right)^{(t-\tau)w} \cdot \left( \mathbb{E}[|e^{-s_2 \beta}|] \right)^{(t-\tau)w},
\end{aligned} \tag{B.12}$$

since  $(\mathbb{E}[|e^{-s \beta}|])^{(t-\tau)w} > 0$ . Hence, the following inequality holds for the right-hand side of Eq. (B.11):

$$\begin{aligned}
& \delta \cdot \frac{\left( \mathbb{E}[e^{-(\delta s_1 + (1-\delta)s_2)\beta}] \right)^{(t-\tau)w}}{1 - (\mathbb{E}[e^{s_1 \alpha}] \cdot \mathbb{E}[e^{-s_1 \beta}])^{t-\tau}} + (1 - \delta) \cdot \frac{\left( \mathbb{E}[e^{-(\delta s_1 + (1-\delta)s_2)\beta}] \right)^{(t-\tau)w}}{1 - (\mathbb{E}[e^{s_2 \alpha}] \cdot \mathbb{E}[e^{-s_2 \beta}])^{t-\tau}} \\
& \leq \delta \cdot \frac{\left( \mathbb{E}[|e^{-s_1 \beta}|] \cdot \mathbb{E}[|e^{-s_2 \beta}|] \right)^{(t-\tau)w}}{1 - (\mathbb{E}[e^{s_1 \alpha}] \cdot \mathbb{E}[e^{-s_1 \beta}])^{t-\tau}} + (1 - \delta) \cdot \frac{\left( \mathbb{E}[|e^{-s_1 \beta}|] \cdot \mathbb{E}[|e^{-s_2 \beta}|] \right)^{(t-\tau)w}}{1 - (\mathbb{E}[e^{s_2 \alpha}] \cdot \mathbb{E}[e^{-s_2 \beta}])^{t-\tau}} \\
& \leq \delta \cdot \frac{\left( \mathbb{E}[|e^{-s_1 \beta}|] \right)^{(t-\tau)w}}{1 - (\mathbb{E}[e^{s_1 \alpha}] \cdot \mathbb{E}[e^{-s_1 \beta}])^{t-\tau}} + (1 - \delta) \cdot \frac{\left( \mathbb{E}[|e^{-s_2 \beta}|] \right)^{(t-\tau)w}}{1 - (\mathbb{E}[e^{s_2 \alpha}] \cdot \mathbb{E}[e^{-s_2 \beta}])^{t-\tau}},
\end{aligned} \tag{B.13}$$

since  $0 \leq (\mathbb{E}[e^{-s_i \beta}])^{(t-\tau)w} \leq 1$  and the Mellin transform of the service is decreasing within the stability interval  $(0, b)$ , reaching the maximal value of 1 for  $s_k = 0, k \in \{1, 2\}$  and  $(t - \tau)w \in \mathbb{Z}$ , guaranteed by the discrete time-domain assumption done in Sec. 3.1. It follows that Eq. (B.9) holds which concludes the delay bound convexity proof.

To prove the second part of Theorem 1, we observe that Eq. (16) defines  $\mathcal{K}^{\mathbb{L}}(s, -w)$  in terms of a recursion starting with the single hop kernel, which is convex in  $s$  according to the first part of the proof above. As  $\mathcal{M}_{g(\gamma)}(1 - s) > 0, \forall s > 0$ , the theorem follows since any positive linear combination of convex functions is also convex [47].

## Bibliography

- [1] ZVEI - German Electrical and Electronic Manufacturers' Association, Coexistence of Wireless Systems in Automation Technology (2009).  
URL <http://www.zvei.org/Publikationen/ZVEI%20Coexistence%20of%20Wireless%20Systems%20in%20Automation%20Technology.pdf>
- [2] R. Berry, Optimal Power-Delay Tradeoffs in Fading Channels - Small-Delay Asymptotics, IEEE Transactions on Information Theory 59 (6) (2013) 3939–3952.
- [3] R. Zheng, R. Kravets, On-demand Power Management for Ad Hoc Networks, Ad Hoc Networks 3 (1) (2005) 51 – 68.

- [4] M. Zafer, E. Modiano, A Calculus Approach to Minimum Energy Transmission Policies with Quality of Service Guarantees, in: INFOCOM 2005. 24th Annual Joint Conference of the IEEE Computer and Communications Societies. Proceedings IEEE, Vol. 1, IEEE, Miami, 2005, pp. 548–559.
- [5] J. Tang, X. Zhang, Cross-Layer-Model Based Adaptive Resource Allocation for Statistical QoS Guarantees in Mobile Wireless Networks, IEEE Transactions on Wireless Communications 7 (6) (2008) 2318–2328.
- [6] S. Kandukuri, S. Boyd, Optimal Power Control in Interference-Limited Fading Wireless Channels with Outage-Probability Specifications, IEEE Transactions on Wireless Communications 1 (1) (2002) 46–55.
- [7] H. Al-Zubaidy, J. Lieberherr, A. Burchard, Network-Layer Performance Analysis of Multi-Hop Fading Channels, IEEE/ACM Transactions on Networking (ToN) 24 (1) (2016) 204–217.
- [8] N. Petreska, H. Al-Zubaidy, R. Knorr, J. Gross, On the Recursive Nature of End-to-End Delay Bound for Heterogeneous Wireless Networks, in: IEEE International Conference on Communications 2015 (ICC 2015), IEEE, London, 2015, pp. 5998–6004.
- [9] U. Kozat, I. Koutsopoulos, L. Tassiulas, Cross-Layer Design for Power Efficiency and QoS Provisioning in Multi-Hop Wireless Networks, Wireless Communications, IEEE Transactions on 5 (11) (2006) 3306–3315.
- [10] R. Cruz, A. Santhanam, Optimal Routing, Link Scheduling and Power Control in Multi-Hop Wireless Networks, in: Proc. INFOCOM 2003., IEEE, San Francisco, 2003, pp. 702–711.
- [11] A. Katsenou, E. Datsika, L. Kondi, E. Papapetrou, K. Parsopoulos, Power-Aware QoS Enhancement in Multihop DS-CDMA Visual Sensor Networks, in: Digital Signal Processing (DSP), 2013 18th International Conference on, IEEE, Fira, 2013, pp. 1–6.
- [12] S. Banerjee, A. Misra, Minimum Energy Paths for Reliable Communication in Multi-hop Wireless Networks, in: MOBIHOC'02, ACM, New York, 2002, pp. 145–156.
- [13] D. Julian, M. Chiang, D. O'Neill, S. Boyd, QoS and Fairness Constrained Convex Optimization of Resource Allocation for Wireless Cellular and Ad Hoc Networks, in: Proc. INFOCOM 2002., Vol. 2, IEE, New York, 2002, pp. 477–486.
- [14] J. Tang, X. Zhang, Power-Delay Tradeoff over Wireless Networks, in: World of Wireless, Mobile and Multimedia Networks, 2008. WoWMoM 2008. 2008 International Symposium on a, IEEE, Newport Beach, CA, 2008, pp. 1–12.

- [15] M. Neely, E. Modiano, C. Rohrs, Dynamic Power Allocation and Routing for Time-Varying Wireless Networks, *IEEE Journal on Selected Areas in Communications* 23 (1) (2005) 89–103.
- [16] Y. Jiang, Y. Liu, *Stochastic Network Calculus*, Springer, USA, 2008.
- [17] Y. Jiang, P. Emstad, Analysis of Stochastic Service Guarantees in Communication Networks: A Traffic Model, Tech. rep., Norwegian University of Science and Technology, Centre for Quantifiable Quality of Service in Communication Systems, Department of Telematics (February 2005).
- [18] M. Fidler, An End-to-End Probabilistic Network Calculus with Moment Generating Functions, in: *Quality of Service, 2006. IWQoS 2006. 14th IEEE International Workshop on*, IEEE, New Haven, CT, 2006, pp. 261–270.
- [19] R. Lubben, M. Fidler, Non-Equilibrium Information Envelopes and the Capacity-Delay-Error-Tradeoff of Source Coding, in: *World of Wireless, Mobile and Multimedia Networks (WoWMoM), 2012 IEEE International Symposium on a*, IEEE, San Francisco, 2012, pp. 1–9.
- [20] M. Fidler, WLC15-2: A Network Calculus Approach to Probabilistic Quality of Service Analysis of Fading Channels, in: *Globecom '06. IEEE*, IEEE, San Francisco, 2006, pp. 1–6.
- [21] F. Ciucu, O. Hohlfeld, P. Hui, Non-Asymptotic Throughput and Delay Distributions in Multi-Hop Wireless Networks, in: *48th Annual Allerton Conference on Communication, Control, and Computing (Allerton)*, IEEE, Illinois, 2010, pp. 662–669.
- [22] F. Ciucu, Non-Asymptotic Capacity and Delay Analysis of Mobile Wireless Networks, *SIGMETRICS Perform. Eval. Rev.* 39 (1) (2011) 359–360.
- [23] F. Ciucu, R. Khalili, Y. Jiang, L. Yang, Y. Cui, Towards a System Theoretic Approach to Wireless Network Capacity in Finite Time and Space, in: *IEEE Infocom*, IEEE, Toronto, 2014, pp. 2391–2399.
- [24] F. Ciucu, A. Burchard, J. Liebeherr, A Network Service Curve Approach for the Stochastic Analysis of Networks, in: *Proceedings of the 2005 ACM SIGMETRICS International Conference on Measurement and Modeling of Computer Systems*, *SIGMETRICS '05*, ACM, New York, 2005, pp. 279–290.
- [25] Y. Hu, H. Li, Z. Chang, Z. Han, End-to-End Backlog and Delay Bound Analysis for Multi-Hop Vehicular Ad Hoc Networks, *IEEE Transactions on Wireless Communications* 16 (10) (2017) 6808–6821.
- [26] F. Poloczek, F. Ciuci, Service-Martingales: Theory and Applications to the Delay Analysis of Random Access Protocols, in: *Proceedings of Computer Communications (INFOCOM), 2015 IEEE Conference on*, IEEE, Hong Kong, 2015, pp. 945–953.

- [27] J. Schmitt, S. Bondorf, W. Poe, The Sensor Network Calculus as Key to the Design of Wireless Sensor Networks with Predictable Performance, *Journal of Sensor and Actuator Networks* 6 (21) (2017) 30.
- [28] Y. Cao, Y. Xue, Y. Cui, Network-Calculus-Based Analysis of Power Management in Video Sensor Networks, in: *Proceedings of Global Telecommunications Conference (GLOBECOM)*, 2007, IEEE, Washington DC, USA, 2007, pp. 981–985.
- [29] W. Y. Poe, M. Beck, J. Schmitt, Achieving High Lifetime and Low Delay in Very Large Sensors Networks using Mobile Sinks, in: *Proceedings of the 8th IEEE International Conference on Distributed Computing in Sensor Systems*, IEEE, Hangzhou, China, 2012, pp. 17–24.
- [30] N. Petreska, H. Al-Zubaidy, J. Gross, Power Minimization for Industrial Wireless Networks under Statistical Delay Constraints, in: *Teletraffic Congress (ITC)*, 2014 26th International, IEEE, Karlskrona, 2014, pp. 1–9.
- [31] R. Knopp, P. Humblet, On Coding for Block Fading Channels, *Information Theory, IEEE Transactions on* 46 (1) (2000) 189–205.
- [32] A. Goldsmith, C. Soon-Ghee, Variable-Rate Variable-Power MQAM for Fading Channels, *Communications, IEEE Transactions on* 45 (10) (1997) 1218–1230.
- [33] W. Dapeng, R. Negi, Effective Capacity: A Wireless Link Model for Support of Quality of Service, *IEEE Transactions Wireless Communications* 2 (4) (2003) 630–643.
- [34] Y. Jiang, P. Emstad, Analysis of Stochastic Service Guarantees in Communication Networks: A Server Model, Tech. rep., Norwegian University of Science and Technology, Centre for Quantifiable Quality of Service in Communication Systems, Department of Telematics (April 2005).
- [35] J. Lee, N. Jindal, Energy-Efficient Scheduling of Delay Constrained Traffic Over Fading Channels, *Wireless Communications, IEEE Transactions on* 8 (4) (2009) 1866–1875.
- [36] K. Mahmood, M. Vehkaperä, Y. Jiang, Delay Constrained Throughput Analysis of a Correlated MIMO Wireless Channel, in: *Computer Communications and Networks (ICCCN)*, 2011 Proceedings of 20th International Conference on, IEEE, Maui, HI, 2011, pp. 1–7.
- [37] B. Davies, *Integral Transforms and Their Applications*, Springer-Verlag, New York, 1978.
- [38] O. Khader, A. Willig, An Energy Consumption Analysis of the Wireless HART TDMA Protocol, *Computer Communications* 36 (7) (2013) 804 – 816.

- [39] Q. Wang, M. Hempstead, W. Yang, A Realistic Power Consumption Model for Wireless Sensor Network Devices, in: *Sensor and Ad Hoc Communications and Networks*, 3rd Annual IEEE Communications Society on, 2006, pp. 286–295.
- [40] L. Feeney, An Energy-Consumption Model for Performance Analysis of Routing Protocols for Mobile Ad Hoc Network, *Mobile Networks and Applications* 6 (3) (2001) 239–249.
- [41] IEEE 802.15.4 WPAN Task Group, 802.15.4-2006 - IEEE Standard for Information technology – Local and metropolitan area networks – Specific requirements – Part 15.4: Wireless Medium Access Control (MAC) and Physical Layer (PHY) Specifications for Low Rate Wireless Personal Area Networks (WPANs) (Jun. 2006).  
URL <https://standards.ieee.org/findstds/standard/802.15.4-2006.html>
- [42] A. Corporation, MCU Wireless AT86RF233 Preliminary Datasheet, Atmel Corporation, 1600 Technology Drive, San Jose, CA 95110 USA (2014).
- [43] H. C. Foundation, *Wirelesshart@technology* (2013).  
URL <http://www.hartcomm.org/>
- [44] N. Petreska, H. Al-Zubaidy, B. Staehle, R. Knorr, J. Gross, Statistical Delay Bound for WirelessHART Networks, in: *Proceedings of the 13th ACM Symposium on Performance Evaluation of Wireless Ad Hoc, Sensor, & Ubiquitous Networks*, ACM, New York, NY, USA, 2016, pp. 33–40.
- [45] I. Florescu, C. Tudor, Appendix B: Inequalities Involving Random Variables and Their Expectations, John Wiley & Sons, Inc., Wiley Online Library, 2013, pp. 434–444.
- [46] S. Boyd, L. Vandenberghe, *Convex Optimization*, Cambridge University Press, Cambridge, UK, 2004.
- [47] F. Clarke, *Functional Analysis, Calculus of Variations and Optimal Control*, Springer-Verlag London, London, UK, 2013.